Acta Crystallographica Section A
Foundations of Crystallography
ISSN 0108-7673

Received 13 June 2003
Accepted 10 November 2003

Time-dependent Takagi–Taupin eikonal theory of X-ray diffraction in rapidly changing crystal structures

Bernhard W. Adams

Argonne National Laboratory, Argonne, IL 60439, USA. Correspondence e-mail: adams@aps.anl.gov

The Takagi–Taupin theory is extended by synthesizing it with the eikonal theory in a unified space–time approach based upon microscopic electromagnetism. The principal goal is the description of X-ray diffraction in a crystal undergoing subpicosecond and few-femtosecond changes.

1. Introduction

The dynamical theory of X-ray diffraction is used for the description of coherent X-ray scattering in large perfect crystals. The theory has been extended in several ways to deal with slight disturbances of the crystal lattice. Most notable among these are: (i) Kato's statistical dynamical diffraction theory (Kato, 1980*a*,*b*); (ii) the ray–optical methods of Penning and Polder (Penning & Polder, 1961; Okkerse & Penning, 1963) and the eikonal theory (Kato, 1963, 1964*a*,*b*; Bonse, 1964; Bonse & Graeff, 1973); and (iii) the wave–optical method of Takagi and Taupin (Takagi, 1962, 1969; Taupin, 1964). All of these extensions were originally formulated for static disturbances of the crystal lattice. Quasistatic disturbances due to, *e.g.*, ultrasound excitation, were also investigated (Entin, 1978; Entin & Assur, 1981; Zolotoyabko & Panov, 1992; Zolotoyabko *et al.*, 1992, 1994; Zolotoyabko & Sander, 1995).

With the motivation of scientific interest and the advent of short-pulse X-ray sources, the focus of interest has recently turned towards time-dependent X-ray diffraction. Most of the science addressed by subpicosecond X-ray pulses is that of the elementary processes of chemistry and condensed matter dynamics, such as molecular or lattice vibrations, non-equilibrium phase transitions and ultimately, at time scales down to a few femtoseconds, the electronic scattering and decoherence times in photoexcited molecules and semiconductors. The scientific cases prepared for the X-ray free-electron laser (XFEL) projects (Materlik & Tschentscher, 2001) give an overview of the science envisioned with short-pulse X-rays. Hard X-rays (defined here as capable of diffraction in typical crystals) of femtosecond duration are currently produced by laser-driven plasma sources or by use of special accelerator techniques, such as bunch slicing (Schoenlein, Chattopadhyay, Chong, Glover, Heimann, Leemans *et al.*, 2000; Schoenlein, Chattopadhyay, Chong, Glover, Heimann, Shank *et al.*, 2000) or extreme bunch compression in the Subpicosecond Pulse Source (SPPS) (Krejcik *et al.*, 2001) at the Stanford Linear Accelerator (SLAC). Another type of accelerator-based source, the Energy-Recovering Linear accelerator (ERL) is currently in the advanced conceptual design phase (Bilderback *et al.*, 2001, 2003).

The science with and the sources of subpicosecond hard X-rays require the development of X-ray optics capable of manipulating and measuring X-rays on the same time scales (Adams, 2002). In principle, it is possible to change the diffractive properties of a crystal within femtoseconds through excitation with an intense laser pulse: optical phonons typically have oscillation periods around 100 fs and the delocalization of the valence electrons (which are the majority in low-Z material like diamond) can occur within a few femtoseconds. This is discussed further in Appendix *C*. Furthermore, with the intensities available from an XFEL, the X-rays themselves can delocalize the electrons of the diffracting material within a few femtoseconds (Neutze *et al.*, 2000). Dynamical diffraction under these conditions requires a theory that takes time dependence explicitly into account.

The work on short-pulse dynamical diffraction can be divided into two categories. The first of these considers the diffraction of a very short X-ray pulse in a perfect-crystal lattice (Wark & He, 1994; Chukhovskii & Förster, 1995; Shastri *et al.*, 2001; Graeff, 2002). 'Very short' in this context means that the corresponding transform-limited spectral width is of the order of, or larger than, the plane-wave energy bandpass of the respective X-ray Bragg reflection. For X-rays at a wavelength of 1 Å and an Si (111) reflection, the bandpass ΔE is about 1.6 eV and the corresponding time $2\pi\hbar/\Delta E$ is 2.6 fs. The other category (Wark & Lee, 1999; Adams, 2002; Sondhauss & Wark, 2003) addresses the problem of X-ray diffraction under the conditions of rapidly variable diffractive properties of the crystal. New phenomena relative to static cases must be expected when the crystal's diffractive properties change markedly within the X-ray/crystal interaction time (see §§12, 13 and Appendix *C*).

The work presented here is a synthesis of the eikonal theory with a time-dependent version of the Takagi–Taupin theory. The principal goal of the theory is to describe X-ray diffraction

under the conditions of a strong subpicosecond (and down to a few femtoseconds) change of the crystal diffractive properties. With the eikonal comes the powerful visual language of dispersion surfaces and whatever is left over by the ray–optical eikonal approximation is taken up by the wave–optical differential equations of the Takagi–Taupin theory. Numerical calculations can be expected to be more precise than within the standard Takagi–Taupin theory because the use of an eikonal has the effect of minimizing the first-order derivatives of the field amplitudes (which is beneficial to numeric calculations) and at the same time implicitly reducing (although not strictly minimizing) the second-order derivatives (which are neglected altogether in Takagi's, though not in Taupin's, formulation).

The theory is developed in a unified space–time approach and is based upon microscopic electromagnetism, using the vector potential $\mathbf{A}$ and the electron density η instead of the macroscopic electric field $\mathbf{D}$ and the electric susceptibility χ. The latter are derived quantities and their meaning needs to be revisited for cases where the crystal is subjected to a strong and rapidly traveling disturbance (see discussion in Appendices *B* and *C*). Instead of doing so, this text stays with microscopic electromagnetism. A microscopic formulation of the dynamical diffraction theory has been used before in the description of magnetic scattering (Davis, 1995) and is also applicable to nonlinear dynamical diffraction (Adams, 2003), which appears in the context of parametric down conversion of X-rays (Adams *et al.*, 2000; Adams, 2003) and will also become relevant with XFELs.

2. The wave equation

By use of the transverse gauge $\nabla \cdot \mathbf{A} = 0$, Maxwell's equations are equivalently expressed as $\nabla^2\Phi = -4\pi\rho$ (henceforth of no further concern), and a wave equation [Jackson, 1975, equation (6.52)]

$$\nabla^2\mathbf{A} - \frac{1}{c^2}\frac{\partial^2\mathbf{A}}{\partial t^2} = -\frac{4\pi}{c}\mathbf{J}_t, \tag{1}$$

where $\mathbf{J}_t$ is the transverse current [Jackson, 1975, equation (6.50)],

$$\mathbf{J}_t(\mathbf{r}) = \frac{1}{4\pi}\nabla \times \nabla \times \int \frac{\mathbf{J}}{|\mathbf{r}-\mathbf{r}'|}\,\mathrm{d}\mathbf{r}'. \tag{2}$$

Although the current $\mathbf{J}$ is generated by the transverse fields, it has a small longitudinal component, which is due to refractive effects in the crystal. However, $\mathbf{J}_t$ is transverse by definition. Furthermore, (2) permits a decomposition of the current into individually transverse parts, according to the Bloch component waves [see equation (10) below].

The current density is $\mathbf{J} = -e\eta\mathbf{v}$, where the electron velocity $\mathbf{v}$ can be determined by use of the Lorentz equation $\dot{\mathbf{v}} = (-e/m)[\mathbf{E} + (1/c)\mathbf{v} \times \mathbf{B}]$. The $\mathbf{v} \times \mathbf{B}$ term contributes only in extreme cases (see Appendix *D*) and Φ gives rise to a small longitudinal current. Both will be ignored here, but see the discussion in Appendix *D* We have then $\mathbf{E} = -\dot{\mathbf{A}}$ and $\dot{\mathbf{v}} = (e/mc)\dot{\mathbf{A}}$. Assuming that the electrons have zero velocity in the absence of electromagnetic waves, the Lorentz equation can be integrated directly to give $\mathbf{v} = (e/mc)\mathbf{A}$.

3. Disturbed lattice

For the following discussion, two types of disturbance will be treated separately. The first of these, henceforth called a lattice distortion, can be desribed by a vector field $\mathbf{u}(\mathbf{r}, t)$, which represents a displacement of the lattice from $\mathbf{r}$ to $\mathbf{r} + \mathbf{u}$. The other, henceforth called a parameter modulation, consists of a change of the diffractive properties of the lattice in space and time, without a change in the lattice itself. The two can appear in combination with each other. Lattice distortions are typically due to static strain or sound waves, while parameter modulations may be caused by optical phonons, polarons, purely electronic excitations (an excitation across the band structure being equivalent to a conversion from bonding to antibonding orbitals).

A rigorous definition of a local reciprocal lattice can be given by describing the distorted lattice as a manifold that is parametrized by the corresponding coordinates of the undistorted lattice (Bishop & Goldberg, 1968). One can then define a local reciprocal lattice (Takagi, 1969) in a point $\mathbf{r} + \mathbf{u}(\mathbf{r})$ of the distorted crystal as a set of points within the tangent space in point $\mathbf{r}$ of the undistorted lattice. For small $\mathbf{u}$, one may approximate the local reciprocal lattice in point $\mathbf{r}$ of the distorted crystal through the tangent space in $\mathbf{r} - \mathbf{u}$. The reciprocal-lattice vectors are the gradients of the lattice phases, *i.e.* a local reciprocal-lattice vector $\mathbf{h}^\circ$ in a point $\mathbf{r}$ of the distorted crystal, corresponding to a reciprocal-lattice vector $\mathbf{h}$ of the undistorted crystal, is given by [Authier, 2001, equation (13.4a)]:

$$\mathbf{h}^\circ = \nabla\{\mathbf{h} \cdot [\mathbf{r} - \mathbf{u}(\mathbf{r})]\} = \mathbf{h} - \nabla\mathbf{u} \cdot \mathbf{h}, \tag{3}$$

and the electron density η of the crystal is

$$\eta(\mathbf{r}, t) = \textstyle\sum_{\mathbf{h}} \tilde{\eta}_{\mathbf{h}}(\mathbf{r}, t)\exp[i\mathbf{h} \cdot (\mathbf{r} - \mathbf{u})]. \tag{4}$$

The electronic contribution to the charge density is then $-e\eta$, which corresponds to the symbol η in the notation of Jackson [1975, equation (6.72)].

A spatio-temporal disturbance of the electron density due to optical phonons, excitons *etc.* can always be decomposed into plane-wave-type elementary disturbances, which are superposed upon the lattice-periodic undisturbed electron density. It is thus convenient for the further development of the theory to model $\eta(\mathbf{r}, t)$ as a sum of distorted (*i.e.* on the background of a lattice distorted by a vector field $\mathbf{u}$) Bloch waves.

$$\begin{aligned} \eta(\mathbf{r}, t) &= \sum_m \sum_{\mathbf{h}} \tilde{\eta}_{m,\mathbf{h}} \exp(i\mathfrak{s}_m)\exp[i\mathbf{h} \cdot (\mathbf{r} - \mathbf{u})], \\ \mathfrak{s}_m &= [\mathfrak{k}_m \cdot (\mathbf{r} - \mathbf{u}) - \varpi_m t], \end{aligned} \tag{5}$$

where $\mathfrak{k}_m$ and ϖ_m are the base vector and the frequency of the mth Bloch wave with $\mathfrak{k}_{-m} = -\mathfrak{k}_m$ and $\varpi_{-m} = -\varpi_m$. The reason for using a Bloch wave here, where, in the standard way of describing phonons (Ashcroft & Mermin, 1976, Chapter 22), a plane-wave representation is sufficient, is the need to

describe a continuous, almost-periodic, electron density, instead of only discrete atom positions.

The terms in (5) with index $m = 0$ represent the electron density of a perfect undisturbed crystal, *i.e.* $\mathfrak{k}_0 = \mathbf{0}$ and $\varpi_0 = 0$. The phase $\mathfrak{s}_m$ is defined relative to the deformed lattice, *i.e.* it contains $\mathfrak{k}_m \cdot (\mathbf{r} - \mathbf{u})$, instead of $\mathfrak{k}_m \cdot \mathbf{r}$ because a modification of the electron density within the unit cells (*i.e.* an optical phonon or a modification in the band/bond structure) is carried along with an overall lattice distortion $\mathbf{u}$. This $\mathbf{r} - \mathbf{u}(\mathbf{r}, t)$ dependence of $\mathfrak{s}_m$ is contained implicitly in the dependence of $\tilde{\eta}_{\mathbf{h}}(\mathbf{r}, t)$ on $\mathbf{r}$ and t.

In practical cases, where one may use laser-generated optical phonons *etc.* in the study of lattice dynamics, or for the coherent subpicosecond manipulation of X-rays (Adams, 2002), usually only a few plane-wave disturbances or a plane-wave-type wave packet of such disturbances will be excited. The Fourier components $\tilde{\eta}_{m,\mathbf{h}}$ can be naturally grouped into sets of four, each containing indices $\pm m$ and $\pm\mathbf{h}$ (except for $m = 0$ and $\mathbf{h}$). Several statements can be made about the members of each set: (i) Any disturbance to the lattice is a real-valued change of the real-valued electron density. Therefore, $\tilde{\eta}_{m,\mathbf{h}}$ and $\tilde{\eta}_{-m,-\mathbf{h}}$ are complex conjugates of each other. (ii) $\tilde{\eta}_{m,\mathbf{h}}$ and $\tilde{\eta}_{-m,\mathbf{h}}$ must have the same modulus, because otherwise the reciprocal lattice would be changed: Take, for example, the extreme case of $\tilde{\eta}_{m,\mathbf{h}} \neq 0$ and $\tilde{\eta}_{-m,\mathbf{h}} = 0$, *i.e.* only two Fourier components, $\tilde{\eta}_{m,\mathbf{h}}$ and $\tilde{\eta}_{-m,-\mathbf{h}}$, are present with exponents $\pm i[(\mathbf{h} + \mathfrak{k}_m) \cdot (\mathbf{r} - \mathbf{u}) - \varpi_m t]$, and the lattice periodicity is actually given by the reciprocal vector $\mathbf{h} + \mathfrak{k}_m$. This is however excluded by definition because lattice parameter changes are to be described by $\mathbf{u}$. (iii) If $\tilde{\eta}_{m,\mathbf{h}} = \tilde{\eta}_{-m,\mathbf{h}}$ for a given $\mathbf{h}$ and all m, then the disturbance does not introduce any inversion asymmetry relative to $\mathbf{h}$ beyond what may already be present in the crystal in the sense that the coordinate origin can then be chosen to make $\tilde{\eta}_{m,\mathbf{h}}$ real-valued for all m. If this coordinate origin is independent of $\mathbf{h}$, then the crystal is inversion symmetric relative to it, and the disturbance does not change that property. (iv) If $\tilde{\eta}_{0,\mathbf{h}} = \tilde{\eta}_{0,-\mathbf{h}}$ for all m, $\mathbf{h}$, then the structure is inversion symmetric in the absence of the disturbance, and that property is preserved under the disturbance only if $\tilde{\eta}_{m,\mathbf{h}} = \tilde{\eta}_{-m,\mathbf{h}}$ and $\tilde{\eta}_{m,\mathbf{h}} = \tilde{\eta}_{m,-\mathbf{h}}$ for all m, $\mathbf{h}$.

For the vector potential, a pair of complex-conjugate modulated Bloch waves $\mathbf{A}(\mathbf{r}, t) = \mathbf{A}^{(+)}(\mathbf{r}, t) + \mathbf{A}^{(-)}(\mathbf{r}, t)$ is used, with

$$\mathbf{A}^{(+)}(\mathbf{r}, t) = \sum_{n=1}^{N} \exp\{i[\mathbf{k_0} \cdot \mathbf{r} - \omega t + \varphi_n(\mathbf{r}, t)]\} \times \sum_{\mathbf{h}} \tilde{\mathbf{A}}_{\mathbf{h}}^{(+,n)}(\mathbf{r}, t) \exp[i\mathbf{h} \cdot (\mathbf{r} - \mathbf{u})]. \quad (6)$$

The phase factor $\exp\{i[\mathbf{k_0} \cdot \mathbf{r} - \omega t + \varphi_n(\mathbf{r}, t)]\}$ applies to all of the Bloch wave and the eikonal, *i.e.* the optical phase, along $\mathbf{k_0} + \nabla\varphi_n$ of the Bloch component wave $(\mathbf{k_0}, \tilde{\mathbf{A}}_{\mathbf{0}})$, is equal to $(\mathbf{k_0} \cdot \mathbf{r} + \varphi_n)/k$, where k is the vacuum wavenumber. The function $\varphi_n(\mathbf{r}, t)$ will henceforth be called the eikonal function. The index n is used to label sets of Bloch waves with different eikonal functions φ_n, which refer to the N branches of the N-wave dispersion surface in the corresponding undisturbed crystal. Solutions with different indices n will be considered separately below, and the index n, as well as the superscript $+$, will be suppressed in the notation, where possible, to reduce the complexity of the formulas.

The Bloch component waves are defined to each fulfil the transverse gauge condition, *i.e.*

$$\nabla \cdot \left(\tilde{\mathbf{A}}_{\mathbf{h}} \exp\{i[\mathbf{k_0} \cdot \mathbf{r} + \varphi + \mathbf{h} \cdot (\mathbf{r} - \mathbf{u})]\}\right) = 0.$$

They are also defined to be transverse themselves at $\mathbf{r} = \mathbf{0}$, *i.e.* $\mathbf{k}_{\mathbf{h}^\circ} \cdot \tilde{\mathbf{A}}_{\mathbf{h}} = 0$ with the abbreviation $\mathbf{k}_{\mathbf{h}^\circ} = \mathbf{k_0} + \mathbf{h} - \nabla\mathbf{u} \cdot \mathbf{h}$. However, in the course of propagation, a wave may develop a longitudinal component (see Appendix *D*), whereupon $\nabla \cdot \tilde{\mathbf{A}}_{\mathbf{h}} \neq 0$ from the transverse gauge condition.

4. The differential equations

Equations (5) and (6) can now be combined to obtain the current density $\mathbf{J} = -e\eta\mathbf{v}$. After application of the index transformation $\mathbf{h} + \mathbf{h}' \rightarrow \mathbf{h}$ and $\mathbf{h}' \rightarrow \mathbf{h}'$, one obtains

$$\mathbf{J}(\mathbf{r}, t) = -r_e c \sum_{\mathbf{h},\mathbf{h}',m} \tilde{\eta}_{m,\mathbf{h}-\mathbf{h}'} \tilde{\mathbf{A}}_{\mathbf{h}'} \exp[i(S_{\mathbf{h}} + \mathfrak{s}_m)], \quad (7)$$

where r_e is the classical electron radius, and the abbreviation

$$S_{\mathbf{h}}(\mathbf{r}, t) = [\mathbf{k_0} \cdot \mathbf{r} + \varphi(\mathbf{r}, t) - \omega t] + \mathbf{h} \cdot (\mathbf{r} - \mathbf{u}) \quad (8)$$

is used.

It is sufficient to regard only the positive-directed waves and currents $\tilde{\mathbf{A}}_{\mathbf{h}}^{(+)}$ and $\mathbf{J}^{(+)}$, and the $(+)$ will be suppressed accordingly. Also, $\mathbf{r}$ and t will henceforth be omitted as arguments to $\tilde{\eta}$, $\tilde{\mathbf{A}}_{\mathbf{h}'}^{(+)}$, $S_{\mathbf{h}}(\mathbf{r}, t)$ and $\mathfrak{s}_m(\mathbf{r}, t)$.

In order to express the integral in equation (2) for the transverse current, we use Taylor expansions up to first order in $\mathbf{r}'$, centered at $\mathbf{r}$ for $\mathbf{h} \cdot \mathbf{u}(\mathbf{r}', t)$, $\varphi(\mathbf{r}', t)$ and $\tilde{\mathbf{A}}'_{\mathbf{h}}$. Details are given in Appendix *A*.

$$\mathbf{J}_t = -r_e c \sum_{\mathbf{h},\mathbf{h}',m} \tilde{\eta}_{m,\mathbf{h}-\mathbf{h}'} \left\{ [\tilde{\mathbf{A}}_{\mathbf{h}'}^{m}]_{\mathbf{h}} + i \frac{[\nabla \tilde{\mathbf{A}}_{\mathbf{h}'}^{(m)}]_{\mathbf{h}}}{k} \right\} \exp[i(S_{\mathbf{h}} + \mathfrak{s}_m)], \quad (9)$$

where

$$[\tilde{\mathbf{A}}_{\mathbf{h}'}^{m}]_{\mathbf{h}} = \frac{\mathfrak{K}_{\mathbf{h},m} \times \tilde{\mathbf{A}}_{\mathbf{h}'} \times \mathfrak{K}_{\mathbf{h},m}}{|\mathfrak{K}_{\mathbf{h},m}|^2}, \quad (10)$$

with $\mathfrak{K}_{\mathbf{h},m} = \mathbf{k}_{\mathbf{h}^\circ} + \mathfrak{k}_m + \nabla\varphi$ and

$$\frac{[\nabla \tilde{\mathbf{A}}_{\mathbf{h}'}^{(m)}]_{\mathbf{h}}}{k} \mathbf{h} = -\frac{\mathfrak{K}_{\mathbf{h},m} \times (\mathfrak{K}_{\mathbf{h},m} \cdot \nabla \tilde{\mathbf{A}}_{\mathbf{h}'}) \times \mathfrak{K}_{\mathbf{h},m}}{|\mathfrak{K}_{\mathbf{h},m}|^4} + 2\frac{\mathfrak{K}_{\mathbf{h},m} \times (\nabla \times \tilde{\mathbf{A}}_{\mathbf{h}})}{|\mathfrak{K}_{\mathbf{h},m}|^2} + \frac{\mathfrak{K}_{\mathbf{h},m}(\nabla \cdot \tilde{\mathbf{A}}_{\mathbf{h}}) - \nabla(\mathfrak{K}_{\mathbf{h},m} \cdot \tilde{\mathbf{A}}_{\mathbf{h}})}{|\mathfrak{K}_{\mathbf{h},m}|^2}. \quad (11)$$

Despite appearances, $[\nabla \tilde{\mathbf{A}}_{\mathbf{h}'}^{(m)}]_{\mathbf{h}}$ is a tensor of first rank. The index m in the symbols on the left-hand sides of equations (10) and (11) will henceforth be suppressed where possible to keep the formula clutter in check.

In the final step of the assembly, equations (5), (6) and (9) are inserted into (1). Here, only the leading-order terms will

be kept, and the following will be neglected: (i) second-order derivatives of $\tilde{\mathbf{A}}$; (ii) products of first-order derivatives of φ and $\mathbf{u}$ with first-order derivatives of $\tilde{\mathbf{A}}$; and (iii) products of derivatives of $\tilde{\mathbf{A}}$ with the electron density, *i.e.* all of equation (11). All these terms are taken up again in Appendix *D*. One now obtains a system of differential equations:

$$2i\left(\frac{k}{c}-\frac{\dot{\varphi}}{c^2}+\frac{\dot{\mathbf{u}}\cdot\mathbf{h}}{c^2}\right)\frac{\partial\tilde{\mathbf{A}}_{\mathbf{h}}}{\partial t}-2i(\mathbf{k}_{\mathbf{h}^\circ}+\nabla\varphi)\cdot\nabla\tilde{\mathbf{A}}_{\mathbf{h}}$$
$$=\left[\left(k-\frac{\dot{\varphi}}{c}+\frac{\dot{\mathbf{u}}\cdot\mathbf{h}}{c}\right)^2-(\mathbf{k}_{\mathbf{h}^\circ}+\nabla\varphi)^2\right]\tilde{\mathbf{A}}_{\mathbf{h}}$$
$$-4\pi r_e\sum_{m,\mathbf{h}'}\tilde{\eta}_{m,\mathbf{h}-\mathbf{h}'}\exp(i\mathfrak{s}_m)[\tilde{\mathbf{A}}_{\mathbf{h}'}]_{\mathbf{h}}. \qquad (12)$$

For any given wavevector $\mathbf{k_0}$ and any given function $\varphi(\mathbf{r}, t)$, this is a system of first-order partial differential equations of hyperbolic type. The function $\varphi(\mathbf{r}, t)$ is not sought as a solution of equation (12). It is an arbitrary function, available (details below) to tune some of the properties of equation (12), which is then solved for the field amplitudes. Equation (12) may be integrated by propagating along the space–time directions given by $\{[k/c-\dot{\varphi}/c^2+(\dot{\mathbf{u}}\cdot\mathbf{h})/c^2], \mathbf{k}_{\mathbf{h}^\circ}-\nabla\varphi\}$.

Equation (12) looks very similar to its counterpart on the basis of macroscopic electromagnetism [see Appendix *B* and equation (16) in Sondhauss & Wark (2003)]. However, the denominator in equation (10) contains $\mathbf{k}_{\mathbf{h}^\circ}+\mathfrak{k}_m+\nabla\varphi$, where the corresponding symbol $[\tilde{\mathbf{D}}_{\mathbf{h}'}]_{\mathbf{h}}$ of the macroscopic formulation contains only k^2. In most cases, $\mathfrak{k}_m$ is very much smaller than $\mathbf{k}_{\mathbf{h}^\circ}$: for example, a laser-induced optical phonon has a wavenumber no larger than the reciprocal laser wavelength. However, a steep disturbance contains large spatial frequencies $|\mathfrak{k}_m|$ and then the difference between k and $\mathbf{k}_{\mathbf{h}^\circ}+\mathfrak{k}_m+\nabla\varphi$ does become important. As long as the disturbance contains only one such spatial frequency, a modified unit cell may be defined, and macroscopic electromagnetism is applicable. Nonetheless, in many cases one encounters a nonperiodic disturbance such as a wavepacket, and then a redefined unit cell cannot be used. Such a wavepacket disturbance, traveling with a group velocity matched to that of the diffracting X-rays, is particularly interesting in the context of the coherent ultrafast manipulation of X-rays, which is the motivation of this text.

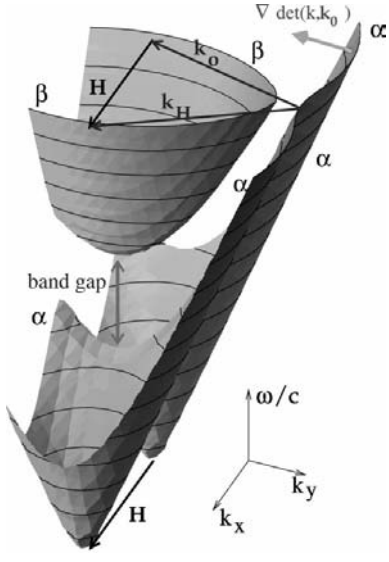

Figure 1
The dispersion surface of the two-wave case in the three-dimensional space of wavenumbers k and wavevector components $\mathbf{k}_x$, $\mathbf{k}_y$. The gradient $\nabla\det(k, \mathbf{k_0})$ gives the propagation direction in space–time of a wavepacket synthesized from the neighborhood of its origin. See text for details.

5. Solutions in a perfect crystal

For an undisturbed perfect crystal, coordinates may be chosen to make $\mathbf{u}$ vanish everywhere, and the sum over $m, \mathbf{h}'$ in equation (12) contains only the terms with $m = 0$. The eikonal function φ may then be made constant in time and space, whereupon the field amplitudes are so, too. That leaves a system of linear equations:

$$0=[k^2-\mathbf{k}_{\mathbf{h}}^2]\tilde{\mathbf{A}}_{\mathbf{h}}-4\pi r_e\sum_{\mathbf{h}'}\tilde{\eta}_{0,\mathbf{h}-\mathbf{h}'}[\tilde{\mathbf{A}}_{\mathbf{h}'}]_{\mathbf{h}}, \qquad (13)$$

which is to be solved for the field amplitudes. Nontrivial solutions are obtained if the determinant $\det(k, \mathbf{k_0})$ of coefficients is zero. This condition defines a three-dimensional surface in the four-dimensional space of wavenumbers and wavevectors (*i.e.* photon energy and momentum). Fig. 1 shows such a surface for the two-wave case (with only two appreciable amplitudes $\tilde{\mathbf{A}}_{\mathbf{0}}$ and $\tilde{\mathbf{A}}_{\mathbf{H}}$, coupled through the reciprocal-lattice vector $\mathbf{H}$), plotted in the three-dimensional space of wavenumber *versus* wavevector components k_x, k_y. The gap between the α and β branches (Batterman & Cole, 1964) is exaggerated. Projected onto the k, k_x plane, it is a photonic band gap (although not omnidirectional like a true band gap) and, projected onto the k_x, k_y plane, it is the gap between the branches of the dispersion hyperbola.

A point on the dispersion surface represents the phase velocities of the waves participating in the diffraction, *i.e.* the wavevectors $\mathbf{k_0}$ and $\mathbf{k_H}$ in Fig. 1 belong to diffractively propagating waves with phase velocities $\omega/|\mathbf{k_0}|$ and $\omega/|\mathbf{k_H}|$, respectively. The group velocity of a diffracting mode is given by $\nabla_{\mathbf{k}}\omega$, which is reciprocal to the slope of the projection of

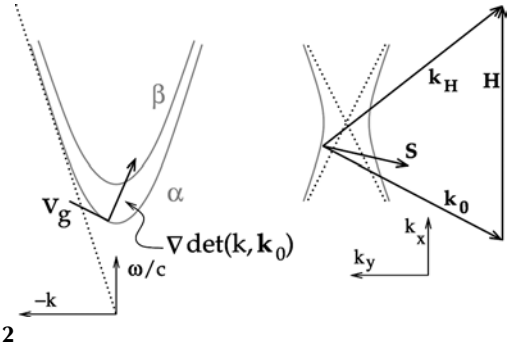

Figure 2
Left: group velocity $\nabla_{\mathbf{k}}\omega$, given by the slope of the line labeled v_g, which is perpendicular to the projection of $\nabla\det(k, \mathbf{k_0})$ onto the momentum-energy coordinates. Right: Poynting vector $\mathbf{S}$ parallel to the projections of $\nabla\det(k, \mathbf{k_0})$ onto the momentum coordinates. See text for details.

$\nabla \det(k, \mathbf{k_0})$ onto a plane containing the energy-momentum coordinates (Fig. 2, left-hand side).

That gradient is, of course, perpendicular to the surface shown in Fig. 1. Projecting it onto the plane containing the momentum coordinates yields a vector that is perpendicular to the dispersion hyperbola, *i.e.* pointing along the Poynting vector (von Laue, 1952; Kato, 1958). Putting these two aspects together yields an interpretation of $\nabla \det(k, \mathbf{k_0})$ as being the direction in space and time of a wavepacket that is synthesized from modes close to its origin on the dispersion surface.

These observations demonstrate how useful dispersion surfaces are and give the incentive for an introduction of this concept into the Takagi–Taupin theory.

Before doing so, however, let us discuss a few points about equation (12) within the simple context of a perfect crystal. These are elementary here but will become important below in the context of a disturbed crystal. If the Bloch base vector $\mathbf{k_0}$ is made to lie on the dispersion surface, then field amplitudes $\tilde{\mathbf{A}}_\mathbf{h}$ exist that solve the system (13) of linear equations. A point on the dispersion surface that makes a set of field amplitudes a solution of equation (13) is called a tie point (Batterman & Cole, 1964). Although a tie point need not exist for any arbitrary set of field amplitudes, a decomposition into sets of amplitudes with tie points on several branches of the dispersion surface can always be found. This will no longer be globally true in a disturbed crystal (see below). Suppose now the Bloch base vector $\mathbf{k_0}$ has been chosen not to lie anywhere on the dispersion surface or that a wrong frequency ϖ has been inserted. Both of these mismatches can be corrected by a judicial choice of $\varphi(\mathbf{r}, t)$, with a constant $\nabla\varphi$ correcting for a wavevector mismatch and a constant $\dot{\varphi}$ correcting for a frequency mismatch. What if $\varphi(\mathbf{r}, t)$ has been chosen incorrectly for that purpose, with $\mathbf{k_0} + \nabla\varphi$ originating from a wrong tie point for a particular set of field amplitudes, or not lying on a dispersion surface at all, or if the field amplitudes are no solution for any tie point? This is shown in Fig. 3: the directional derivatives of the field amplitudes on the left-hand side of equation (12) now take up the mismatch, with the second-order tensor $i\nabla\tilde{\mathbf{A}}_\mathbf{h}$ compensating for a mismatch in the tensor $(\mathbf{k_h} + \nabla\varphi) \otimes \tilde{\mathbf{A}}_\mathbf{h}$ [where $\otimes$ signifies the tensor product (Bishop & Goldberg, 1968, p. 76)] and with $i(\partial/\partial t)\tilde{\mathbf{A}}_\mathbf{h}$ compensating for $(\omega + \dot{\varphi})\tilde{\mathbf{A}}_\mathbf{h}$.

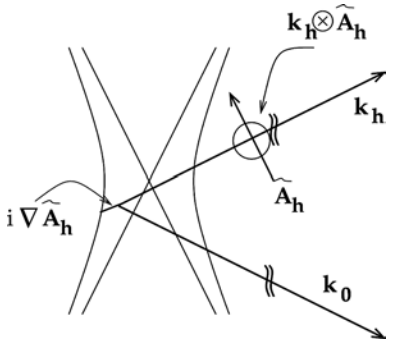

Figure 3
Equivalence of the tensor $i\nabla\tilde{\mathbf{A}}_\mathbf{h}$ to the tensor $\mathbf{k_h} \otimes \tilde{\mathbf{A}}_\mathbf{h}$. The gradient may, of course, also have a component perpendicular to $\mathbf{k_h}$.

The eikonal function can thus be used to minimize the directional derivatives of the field amplitudes. This is trivial in an undisturbed crystal and can be done in an optimization procedure for a disturbed crystal (see below).

6. Disturbed crystal

As demonstrated above, the magnitude of the field amplitude derivatives in equation (12) depends on $\nabla\varphi$ and $\dot{\varphi}$, and the derivatives vanish if $\mathbf{k_0} + \nabla\varphi$ originates from a tie point for a frequency $\omega + \dot{\varphi}$. In a disturbed crystal, tie points cannot be matched everywhere, and one must, instead, minimize the derivatives and approximate the tie points. To that purpose, a merit function is required, whose nature depends on the emphasis (good match throughout the crystal, better match at the surfaces *etc.*). A generic merit function is

$$\int \mathrm{d}\mathbf{r} \left| \sum_\mathbf{h} \left(\mathbf{k_h} \cdot \nabla\tilde{\mathbf{A}}_\mathbf{h}^{(+)} - \frac{k}{c}\frac{\partial\tilde{\mathbf{A}}_\mathbf{h}^{(+)}}{\partial t} \right) \cdot \tilde{\mathbf{A}}_{-\mathbf{h}}^{(-)} \right|, \qquad (14)$$

which weights the derivatives according to the amplitudes themselves and places no particular emphasis on any location or time within the crystal.

The eikonal may now be varied to minimize the merit function. In a numerical procedure, this might be done by interpolating φ between a number of support points $\{s_n, n = 1, \ldots, N\}$ in space and time and varying φ in the s_n. Equation (12) [or actually equation (15) below] is then solved for each set of values of φ in $\{s_n, n = 1, \ldots, N\}$, whereupon the merit function can be evaluated.

The need to transport the field amplitudes within a disturbed crystal and the restriction of $\nabla\varphi$ and $\dot{\varphi}$ being derived from a scalar φ makes it impossible to match the tie points exactly throughout the crystal: a set of field amplitudes that is a solution for a local dispersion surface somewhere in the crystal can evolve into one that has no tie point at all. This point will be taken up again in §11. The eikonal theory ignores this transport issue and assumes that tie points (which are permitted to slide along the dispersion surface) are matched exactly everywhere in the crystal (Kato, 1973). Besides minimizing the field amplitude derivatives, which is of benefit to numerical calculations, the eikonal function used here at the same time makes the dispersion surfaces available in an optimal approximation. Other than in the pure eikonal theory, any mismatch from a local tie point is taken up by the derivatives of the field amplitudes in the way of the original Takagi–Taupin theory.

One is totally free to choose any Bloch base vector $\mathbf{k_0}$ and wavenumber k in equation (12) because the minimization of the merit function (14) will supply the proper eikonal function. However, in the interest of keeping $\nabla\varphi$ and $\dot{\varphi}$ small, $\mathbf{k_0}$ should be chosen to originate from a point that would also be chosen within the standard Takagi–Taupin theory, *i.e.* dispersion hyperbola in Fig. 3, and k should be the refraction-corrected vacuum wavenumber of the incident X-rays. Then, $\nabla\varphi$ is smaller than $\mathbf{k_h}$ by a factor of 10^{-5} or less and, even if the crystal structure should change completely within a few

femtoseconds (which definitely is within the scope of the present theory), $\dot{\varphi}$ is smaller than k by a factor of 10^{-4}. The term $\dot{\mathbf{u}}\cdot\mathbf{h}/c^2$ is even smaller than that. It is thus permissible to approximate equation (12) as

$$\begin{aligned}2i\frac{k}{c}\frac{\partial\tilde{\mathbf{A}}_{\mathbf{h}}}{\partial t} - 2i\mathbf{k}_{\mathbf{h}}\cdot\nabla\tilde{\mathbf{A}}_{\mathbf{h}} &= \left[\left(k-\frac{\dot{\varphi}}{c}\right)^2 - (\mathbf{k}_{\mathbf{h}}+\nabla\varphi)^2\right]\tilde{\mathbf{A}}_{\mathbf{h}} - 4\pi r_e\sum_{m,\mathbf{h}'}\tilde{\eta}_{m,\mathbf{h}-\mathbf{h}'}[\tilde{\mathbf{A}}_{\mathbf{h}'}]_{\mathbf{h}} \\ &\quad + 2\left[\frac{k}{c}\dot{\mathbf{u}}\cdot\mathbf{h} + \mathbf{k}_{\mathbf{h}}\cdot\nabla\mathbf{u}\cdot\mathbf{h}\right]\tilde{\mathbf{A}}_{\mathbf{h}} \\ &\quad - 4\pi r_e\sum_{m,\mathbf{h}'}[\exp(i\mathfrak{s}_m)-1]\tilde{\eta}_{m,\mathbf{h}-\mathbf{h}'}[\tilde{\mathbf{A}}_{\mathbf{h}'}]_{\mathbf{h}}. \qquad (15)\end{aligned}$$

The second line of this equation is directly equivalent to equation (13), and the third line contains all the perturbation terms. If a tie point is matched locally, the second line vanishes, and the perturbations in the third line are equated to the derivatives of the field amplitudes in the first line. Most of the following qualitative arguments will be based upon this observation.

7. Example: static lattice distortion

To illustrate the role of the eikonal function, consider the case of a static lattice deformation, given by a vector field $\mathbf{u}$. Take a set of field amplitudes for which a tie point exists locally at *e.g.* a point on the surface through which the X-rays enter the crystal. Such a set can always be found by splitting *locally* the actual field amplitudes among the branches of the local dispersion surface. In the absence of $\nabla\mathbf{u}$, choose an eikonal function φ_0 so that $\nabla\varphi_0+\mathbf{k_0}$ originates from that tie point [the index 0 is not to be confused with the index n in the definition, equation (6)]. Then 'turn on' $\nabla\mathbf{u}$. Because $\nabla\mathbf{u}\cdot\mathbf{h}$ are different gradients for different reciprocal-lattice vectors $\mathbf{h}$, no eikonal function φ can be found, so that $\nabla\varphi$ compensates for all of them. Although φ cannot be made to fully counter the effect of $\nabla\mathbf{u}$, it can be chosen to make the sum in the integrand of the merit function (14) vanish locally: By multiplying each line in equation (15) with the respective complex conjugate field amplitude and making use of the fact that $\mathbf{k_0}+\nabla\varphi_0$ originates from a tie point, the following two equations are obtained [superscript (+) dropped where possible]:

$$2i\mathbf{k_0}\cdot\nabla\tilde{\mathbf{A}}_{\mathbf{h}}^{(+)}\cdot\tilde{\mathbf{A}}_{-\mathbf{h}}^{(-)} = |\tilde{\mathbf{A}}_{\mathbf{h}}|^2\mathbf{k}_{\mathbf{h}}\cdot[\nabla(\varphi-\varphi_0)-\nabla\mathbf{u}\cdot\mathbf{h}]. \qquad (16)$$

Taking the sum over $\mathbf{h}$ and demanding that the left-hand side [*i.e.* the integrand of equation (14)] vanish gives an equation for $\nabla(\varphi-\varphi_0)$:

$$\left(\sum_{\mathbf{h}}\mathbf{k}_{\mathbf{h}}|\tilde{\mathbf{A}}_{\mathbf{h}}|^2\right)\cdot\nabla(\varphi-\varphi_0) = \sum_{\mathbf{h}}\mathbf{k}_{\mathbf{h}}|\tilde{\mathbf{A}}_{\mathbf{h}}|^2\cdot\nabla\mathbf{u}\cdot\mathbf{h}, \qquad (17)$$

which means that $\nabla(\varphi-\varphi_0)$ interpolates among the gradients $\nabla(\mathbf{u}\cdot\mathbf{h})$. Locally, this interpolation can be expressed in terms of a single gradient $\nabla(\varphi-\varphi_0)$ but globally this is not possible because the field amplitudes $\tilde{\mathbf{A}}_{\mathbf{h}}$ are variable. Equation (17) is discussed further in §10.

8. Comparison with the Takagi–Taupin theory

Other than in the present text, the original Takagi–Taupin theory does not make use of dispersion surfaces and it was derived for static or quasistatic disturbances of the crystal lattice. More recently, the theory was extended to deal with time-dependent lattice disturbances (Adams, 2002; Sondhauss & Wark, 2003). To illustrate the difference between the present theory and the standard Takagi–Taupin theory with regard to a dispersion surface, one might write the dielectric function of the disturbed crystal as $\varepsilon = 1+\chi_p(\mathbf{r})+\chi_d(\mathbf{r},t)$, where χ_p is the spatially periodic susceptibility of the undisturbed crystal and $\chi_d(\mathbf{r},t)$ is due to the disturbance (the macroscopic concept of a dielectric function is only used here to facilitate the comparison with the original Takagi–Taupin theory).

The Takagi–Taupin theory works with field amplitudes $\mathcal{E}_{\mathbf{h}}(\mathbf{r},t)$ in the form $\mathbf{E}^{\mathrm{T}}_{\mathbf{h}}(\mathbf{r})\exp[i(\mathbf{k}_{\mathbf{h}}\cdot\mathbf{r}-\omega t)]$, with $\mathbf{k}_{\mathbf{h}}$ corresponding to the '1' in ε and the remainder $\mathbf{E}^{\mathrm{T}}$ of the spatial dependence of $\mathcal{E}_{\mathbf{h}}$, corresponding to $\chi_p+\chi_d$ in ε, left to be determined in a differential equation. In another approach (Balibar, 1969; Authier & Balibar, 1970), the field amplitudes are written as $\mathbf{E}^{\mathrm{B}}_{\mathbf{h},n}(\mathbf{r})\exp[i(\mathbf{k}_{\mathbf{h},n}\cdot\mathbf{r}-\omega t)]$ (although the index n for the branch of the dispersion surface is omitted there), where $\mathbf{k}_{\mathbf{h},n}$ now originates from a tie point and a full description of the fields in the crystal requires as many $\mathbf{k}_{\mathbf{h},n}$ as there are branches of the dispersion surface. The differential equations now must be solved for $\mathbf{E}^{\mathrm{B}}_{n,\mathbf{h}}$, which corresponds to only χ_d in ε, whereas the part corresponding to $1+\chi_p$ need not be solved for.

In the present theory, $\mathcal{E}_{\mathbf{h}}$ are written as $\mathbf{E}^{\mathrm{E}}_{\mathbf{h},n}(\mathbf{r})\exp[i(\mathbf{k}_{\mathbf{h}}\cdot\mathbf{r}-\omega t+\varphi_n)]$, with the contribution to $\mathcal{E}$, to be determined through a differential equation, corresponding to only part of χ_d. The terms due to '1', 'χ_p' and part of 'χ_d' are removed from the solution. Fig. 4 illustrates the differences between the standard Takagi–Taupin theory (STT), Balibar's approach and the theory presented here (ETT).

9. Comparison with Kato's eikonal theory

Fermat's principle of extremal optical path length can be applied to the diffraction of X-rays (Kato, 1963, 1964*a*,*b*). Starting from a modulated Bloch wave (in the notation of this text),

$$\mathbf{D}(\mathbf{r},t) = \exp(ikS_0)\sum_{\mathbf{h}}\mathbf{D}_{\mathbf{h}}\exp(i\mathbf{h}\cdot\mathbf{r}), \qquad (18)$$

and using the properties of the perfect-crystal dispersion surface, a variational principle and a differential equation to describe the beam trajectories are derived. The variational principle for a beam trajectory from A to B is obtained by use of the convex/concave shapes of the branches of the dispersion surface [Kato, 1963, equation (44)]:

$$\delta\int_A^B(\mathbf{k_0}\cdot\mathrm{d}\mathbf{r}) = 0, \qquad (19)$$

which leads to the Euler–Lagrange equation [Kato, 1963, equation (45)]. Using the property of the dispersion surface

that the Poynting vector is perpendicular to it, this is converted to [Kato, 1963, equation (47)]

$$\frac{\mathrm{d}}{\mathrm{d}\ell}\mathbf{k}_{\mathbf{0},\ell} = \frac{\partial \mathbf{k}_{\mathbf{0}}}{\partial \ell}\cdot\mathbf{n}, \tag{20}$$

where ℓ parametrizes the trajectory, $\mathbf{k}_{\mathbf{0},\ell}$ is the component of $\mathbf{k}_{\mathbf{0}}$ along the trajectory and $\mathbf{n}$ is a normal vector to the dispersion surface. Furthermore, making use of energy conservation (and thus excluding interbranch scattering, see §10), the beam trajectory is related to the energy flow [Kato, 1963, equation (50)].

As stated in the definition of φ, the eikonal in the present theory is actually $(\mathbf{k}_{\mathbf{0}}\cdot\mathbf{r}+\varphi)/k$ and φ itself is called the 'eikonal function'. Strictly speaking, even $(\mathbf{k}_{\mathbf{0}}\cdot\mathbf{r}+\varphi)/k$ is not an eikonal because it does not necessarily take up *all* of the phase of the Bloch wave. In a strong disturbance, the phases of the individual field amplitudes do not evolve by the same amount in the course of propagation and no single eikonal could subsume them. It is exactly this admission of some amount of individual phase evolution of the field amplitudes that makes the present theory applicable to strong disturbances. As a consequence of the departure from a strict eikonal, the present theory cannot make use of the properties of the dispersion surface in an exact sense. Instead, properties of the solutions of the differential equation (15) after the choice of an optimal eikonal function will be discussed in the following sections, and it will be shown that they behave approximately as one would expect from standard dynamical diffraction theory.

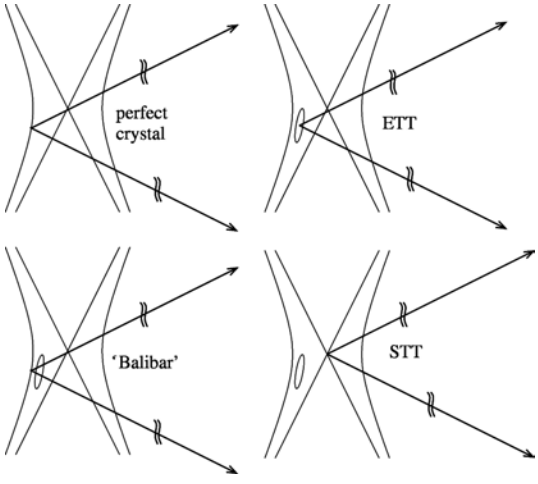

Figure 4
Definitions of the wavevectors in the two-wave case. Upper left: in the perfect-crystal theory, the wavevectors originate from a tie point. Upper right: in the theory presented here, there is no well defined tie point, but modes can be defined, each of which has a tie region (indicated by the ellipse), which is given by the wavevector $\mathbf{k}_{\mathbf{h}}+\nabla\varphi_n$, with φ_n determined through equation (14). The wavevectors are variable through $\nabla\varphi_n$. Lower right: in the standard Takagi–Taupin theory (STT), the wavevectors are fixed and usually originate from the symmetry point of the dispersion hyperbola. Lower left: in Balibar's approach, the wavevectors originate from a fixed tie point of the locally approximated dispersion surface. This tie point is generally close to the tie region of the ETT.

10. Interbranch scattering

Before considering the individual field amplitudes, let us look at the evolution of a diffracting mode as an entity: If, for each $\mathbf{h}$, equation (15) is multiplied with $\tilde{\mathbf{A}}^{(-)}_{-\mathbf{h}}$, the sum over $\mathbf{h}$ is taken and only the lowest order of $\exp(i\mathfrak{s}_m)-1$ is kept, then the left-hand side reads

$$\begin{aligned}
&-2i\sum_{\mathbf{h}}(\mathbf{k}_{\mathbf{h}}\cdot\nabla\tilde{\mathbf{A}}^{(+)}_{\mathbf{h}})\cdot\tilde{\mathbf{A}}^{(-)}_{-\mathbf{h}} + 2i\frac{k}{c}\sum_{\mathbf{h}}\frac{\partial\tilde{\mathbf{A}}^{(+)}_{\mathbf{h}}}{\partial t}\tilde{\mathbf{A}}^{(-)}_{-\mathbf{h}}\\
&\quad=\sum_{\mathbf{h}}\left[\left(k-\frac{\dot{\varphi}}{c}\right)^2-(\mathbf{k}_{\mathbf{h}}+\nabla\varphi)^2\right]|\tilde{\mathbf{A}}_{\mathbf{h}}|^2\\
&\qquad-4\pi r_e\sum_{\substack{m,\mathbf{h}'\\ \mathbf{h}}}\tilde{\eta}_{m,\mathbf{h}-\mathbf{h}'}[\tilde{\mathbf{A}}_{\mathbf{h}'}]_{\mathbf{h}}\tilde{\mathbf{A}}^{(-)}_{-\mathbf{h}}\\
&\qquad+2\sum_{\mathbf{h}}\left[\frac{k}{c}\dot{\mathbf{u}}+\mathbf{k}_{\mathbf{h}}\cdot\nabla\mathbf{u}\right]\cdot\mathbf{h}|\tilde{\mathbf{A}}_{\mathbf{h}}|^2\\
&\qquad-4i\pi r_e\sum_{\substack{m,\mathbf{h}'\\ \mathbf{h}}}\mathfrak{s}_m\tilde{\eta}_{m,\mathbf{h}-\mathbf{h}'}[\tilde{\mathbf{A}}_{\mathbf{h}'}]_{\mathbf{h}}\tilde{\mathbf{A}}^{(-)}_{-\mathbf{h}}.
\end{aligned}\tag{21}$$

The left-hand side (first line) is just the integrand of the merit function (14). It is also the continuity equation of the electromagnetic energy density and flow:

$$-i\frac{4\pi}{kc}\nabla\cdot\mathbf{S}+i\frac{4\pi}{kc}\frac{\partial\mathcal{U}}{\partial t}=(\text{r.h.s.}),\qquad \begin{aligned}\mathbf{S}&=\frac{kc}{4\pi}\sum_{\mathbf{h}}\mathbf{k}_{\mathbf{h}}|\tilde{\mathbf{A}}_{\mathbf{h}}|^2\\ \mathcal{U}&=\frac{k^2}{4\pi}\sum_{\mathbf{h}}|\tilde{\mathbf{A}}_{\mathbf{h}}|^2,\end{aligned}\tag{22}$$

where $\mathbf{S}$ is the Poynting vector [Jackson, 1975, equation (6.109)] and $\mathcal{U}$ is the energy density [Jackson, 1975, equation (6.106)] of the electromagnetic waves represented by the field amplitudes $\tilde{\mathbf{A}}_{\mathbf{h}}$. The abbreviation (r.h.s.) means the right-hand side of equation (21), which contains contributions from the disturbance terms in the third line of equation (21) and also from a possible mismatch of $\mathbf{k}_{\mathbf{0}}+\nabla\varphi$ from the tie point for the amplitudes $\tilde{\mathbf{A}}_{\mathbf{h}}$ (supposing the amplitudes permit a tie point at all, see above).

A nonvanishing divergence means that $\mathbf{S}$ changes its length, which may be due to absorption or also due to the so-called interbranch scattering (Balibar *et al.*, 1983; Kulda, 1984), *i.e.* a reassignment of photons among the modes of dynamical diffraction (branches of the dispersion surface). It should be emphasized here that these modes and the scattering between them are not anything intrinsic to the nature of the problem, because (r.h.s) in equation (22) depends on the choice of φ. There is, however, a minimal scattering rate between the branches, which is obtained by minimizing the merit function (14).

If the eikonal function φ makes $\mathbf{k}_{\mathbf{0}}+\nabla\varphi$ originate from a local tie point, then the second line in equation (21) vanishes, and the disturbances in the third line of equation (21) are directly the driving terms of the continuity equation for $\mathbf{S}$. A change in $\mathbf{S}$ that does not contribute to $\nabla\cdot\mathbf{S}$ changes the direction of $\mathbf{S}$ and, correspondingly, the location of the tie point on the dispersion surface. This is the regime of the

original eikonal theory. If, however, the field amplitudes change in a way that does not admit a tie point, then $\nabla \cdot \mathbf{S} \neq 0$ and interbranch scattering occurs.

In the simple case of an undisturbed crystal, it is possible to relate $\nabla \cdot \mathbf{S}$ directly to a mismatch from a tie point T. Suppose that $\mathbf{k_0} + \nabla\varphi_0$ originates from T but $\mathbf{k_0} + \nabla\varphi$ does not. Neglecting $\dot{\varphi}^2$ and $(\nabla\varphi)^2$, equation (21) can be written as

$$i\frac{\partial \mathcal{U}}{\partial t} - i\nabla \cdot \mathbf{S} = 2(\dot{\varphi} - \dot{\varphi}_0)\mathcal{U} - 2\mathbf{S} \cdot \nabla(\varphi - \varphi_0). \qquad (23)$$

In the presence of a disturbance, there are additional driving terms to the derivatives of $\mathcal{U}$ and $\mathbf{S}$ from the third line of equation (21).

Consider now a disturbed crystal and assume that the field amplitudes at a given point $\mathbf{r}, t$ admit a tie point T and $\mathbf{k_0} + \nabla\varphi_0$ originates from it. Equation (21) then reads:

$$i\frac{\partial \mathcal{U}}{\partial t} - i\nabla \cdot \mathbf{S} = \frac{k^2}{4\pi}\sum_{\mathbf{h}}\left[\dot{\mathbf{u}} + \frac{c}{k}\mathbf{k_h} \cdot \nabla\mathbf{u}\right] \cdot \mathbf{h}|\tilde{\mathbf{A}}_\mathbf{h}|^2 - ikcr_e \sum_{\substack{m,\mathbf{h}' \\ \mathbf{h}}} \mathfrak{s}_m \tilde{\eta}_{m,\mathbf{h}-\mathbf{h}'}[\tilde{\mathbf{A}}_{\mathbf{h}'}]_\mathbf{h}\tilde{\mathbf{A}}^{(-)}_{-\mathbf{h}}. \qquad (24)$$

The lattice disturbance is thus the cause of a sink or source to the continuity equation of the electromagnetic energy flow for a particular branch of the dispersion surface and, in the absence of absorption, this must be attributed to interbranch scattering.

Please note the different but complementary ways of reasoning here and for equation (17). Here, the eikonal function φ_0 that matches the tie point for the amplitudes is kept and the effect of a disturbance on the field amplitudes is studied. For equation (17), another eikonal function φ was chosen to make the sum of the derivatives vanish and equation (17) then gives the projection of $\nabla(\varphi - \varphi_0)$ onto $\mathbf{S}$. Equation (17), supplemented with the time-dependent and the $\tilde{\eta}_{m,\mathbf{h}}$ terms, is:

$$\mathcal{U}(\dot{\varphi} - \dot{\varphi}_0) + \mathbf{S} \cdot \nabla(\varphi - \varphi_0) = \frac{k^2}{4\pi}\sum_{\mathbf{h}}|\tilde{\mathbf{A}}_\mathbf{h}|^2\dot{\mathbf{u}} \cdot \mathbf{h} + \frac{kc}{4\pi}\sum_{\mathbf{h}}\mathbf{k_h}|\tilde{\mathbf{A}}_\mathbf{h}|^2 \cdot \nabla\mathbf{u} \cdot \mathbf{h} - i\frac{kc}{2}r_e \sum_{\substack{m,\mathbf{h}' \\ \mathbf{h}}} \mathfrak{s}_m \tilde{\eta}_{m,\mathbf{h}-\mathbf{h}'}[\tilde{\mathbf{A}}_{\mathbf{h}'}]_\mathbf{h}\tilde{\mathbf{A}}^{(-)}_{-\mathbf{h}}. \qquad (25)$$

11. Static distortion, guided waves, beam stability

For a static deformation, equation (15) is reduced to

$$\mathbf{k_h} \cdot \nabla\tilde{\mathbf{A}}_\mathbf{h} = \frac{i}{2}[k^2 - (\mathbf{k_h} + \nabla\varphi)^2]\tilde{\mathbf{A}}_\mathbf{h} - 2\pi i r_e \sum_{\mathbf{h}'}\tilde{\eta}_{0,\mathbf{h}-\mathbf{h}'}[\tilde{\mathbf{A}}_{\mathbf{h}'}]_\mathbf{h} + i\mathbf{k_h} \cdot \nabla\mathbf{u} \cdot \mathbf{h}\tilde{\mathbf{A}}_\mathbf{h}, \qquad (26)$$

where $\mathbf{h}$ and $\mathbf{h}'$ may take the values $\mathbf{0}$ and $\mathbf{H}$.

We now consider the stability of a mode by following the evolution of the field amplitudes in the course of propagation. The stages of the amplitude evolution in the following discussion are given letters (a), (b), (c), ..., which correspond to the phasors in Fig. 5.

Without loss of generality, assume that the phase of $\tilde{\mathbf{A}}_\mathbf{0}$ at some point $\mathbf{r}$ equals zero and $\tilde{\mathbf{A}}_\mathbf{H} = -\tilde{\mathbf{A}}_\mathbf{0}$ [(a) in Fig. 5], with the wavevector $\mathbf{k_0} + \nabla\varphi$ perfectly matching the tie point on the α branch of the dispersion surface. Then, the right-hand side in the first line of equation (26) vanishes and, with the lattice distortion shown in Fig. 5, the perturbation term $\mathbf{k_H} \cdot \nabla\mathbf{u} \cdot \mathbf{H}$ is negative, while $\mathbf{k_0} \cdot \nabla\mathbf{u} \cdot \mathbf{0}$ is, of course, zero. At a point $\mathbf{r}$ within the crystal, the amplitudes are therefore as shown in (b) in Fig. 5: no change in $\tilde{\mathbf{A}}_\mathbf{0}$ and $\tilde{\mathbf{A}}_\mathbf{H}$ has picked up a negative phase ϕ.

This negative phase of $\tilde{\mathbf{A}}_\mathbf{H}$ makes the sum in the line for $\mathbf{h} = \mathbf{0}$ in equation (26) equal to a real number times a factor $\exp[i(\pi - \phi)] \approx -1 + i\phi$ (with π for the α branch). With the factor $-i$ before the sum and $\tilde{\eta}_\mathbf{H} > 0$ (electron density, not charge density), the directional derivative of $\tilde{\mathbf{A}}_\mathbf{0}$ on the left-hand side acquires a positive real part. Therefore, in the course of propagation, the modulus of $\tilde{\mathbf{A}}_\mathbf{0}$ grows and, with a similar argument, the modulus of $\tilde{\mathbf{A}}_\mathbf{H}$ shrinks [(c) in Fig. 5]. Again, in the line of equation (26) for $\mathbf{h} = \mathbf{0}$, the modulus of the sum is now smaller. The sum is negative owing to the factor $\exp(i\pi)$ between the field amplitudes on the α branch. Therefore, owing to the factor $-i$ before the sum, the right-hand side acquires a negative imaginary part [(d) in Fig. 5]. Likewise, the right-hand side of equation (26) for $\mathbf{h} = \mathbf{H}$ – after multiplying both sides with the phase factor $\exp(-i\pi)$ to cancel the phase $\exp(i\pi)$ of $\tilde{\mathbf{A}}_\mathbf{H}$ – acquires a positive imaginary part (d). This tends to counter the negative phase ϕ that $\tilde{\mathbf{A}}_\mathbf{H}$ started out with. In conclusion, a mode on the α branch is stable with respect to small perturbations and the maxima of the standing waves tend to stay between the lattice planes. This is to be expected because a mode on the α branch has longer wavevectors than one on the β branch and therefore tends to be guided by a refractive index profile (just like light in a glass fiber). Similarly, the evolution of the amplitudes

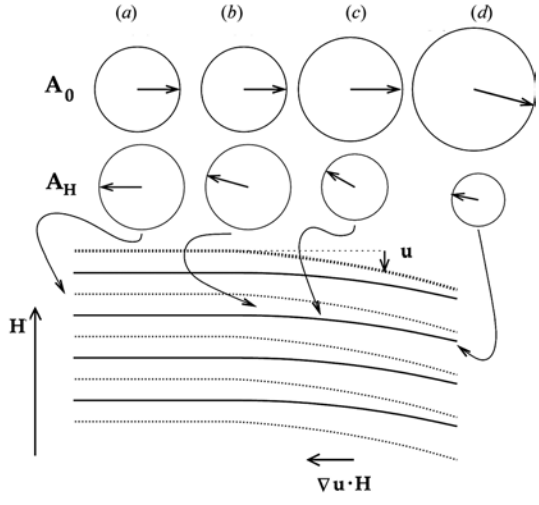

Figure 5
Amplitude evolution, guided waves on the α branch in a distorted crystal. The little phasors for $\tilde{\mathbf{A}}_\mathbf{0}$ and $\tilde{\mathbf{A}}_\mathbf{H}$ have letters (a), (b), (c), ..., which denote stages in the amplitude evolution explained in the text.

can be followed through for the β branch, with the result of a β mode being *unstable* towards small perturbations.

There is of course a limit to the stability of a mode on the α branch. If the disturbance is so strong that the diffractive properties change significantly over the *Pendellösung* length, then guidance of the standing waves breaks down. A quantitative criterion is obtained from equation (26). For stability,

$$\mathbf{k}_\mathbf{h} \cdot \nabla\mathbf{u} \cdot \mathbf{h}\tilde{\mathbf{A}}_\mathbf{h} \ll r_e \sum_{\mathbf{h}'} \tilde{\eta}_{\mathbf{h}-\mathbf{h}'}[\tilde{\mathbf{A}}_{\mathbf{h}'}]_\mathbf{h} \tag{27}$$

must be valid. This expression depends on the magnitude of $\mathbf{u}$ *versus* η and on the amplitude ratios.

The above discussion was about the phases of the field amplitudes and the positions of the standing waves relative to the lattice planes. What about the direction of energy flow, *i.e.* the beams? According to the above discussion for the α branch, the modulus of $\tilde{\mathbf{A}}_\mathbf{0}$ grows at the expense of that of $\tilde{\mathbf{A}}_\mathbf{H}$, as the radiation propagates in a crystal with a curvature as shown in Fig. 5. Therefore, the tie point slides down on the dispersion surface and the beam direction bends downward, *i.e.* with the same tendency as the curvature of the lattice planes. This result was also obtained before (Penning & Polder, 1961) on the basis of geometrical optics [see Fig. 4 of Penning & Polder (1961) and also Fig. 13.10 of Authier (2001)] and has been shown computationally on the basis of the Takagi–Taupin theory (Balibar *et al.*, 1975).

If the crystal deformation is small by the criterion of equation (27), a mode on the α branch will stay there and will only slide along the dispersion surface. This is the regime where the eikonal approximation is applicable. For a stronger deformation or for a mode on the β branch, interbranch scattering occurs and the pure eikonal theory is no longer applicable. However, the eikonal Takagi–Taupin theory presented here can still be used because the differential equations can 'mop up any spills' of the eikonal.

12. Optical phonons, frequency shifts

In this example, a spatially perfect crystal is subjected to a sudden perturbation that induces a rapid change in the electron density but no lattice distortion, *i.e.* $\nabla\mathbf{u} = \mathbf{0}$. An example would be a laser-pulse-induced strongly excited optical phonon. A diffracting mode will have an eikonal function $\varphi_0(\mathbf{r})$ that matches the appropriate tie point perfectly in the absence of the disturbance. Because the unperturbed crystal is static, φ_0 is independent of time. This makes

$$[k^2 - (\mathbf{k}_\mathbf{h} + \nabla\varphi_0)^2]\tilde{\mathbf{A}}_\mathbf{h} - 4\pi r_e \sum_{m,\mathbf{h}'} \tilde{\eta}_{m,\mathbf{h}-\mathbf{h}'}[\tilde{\mathbf{A}}_{\mathbf{h}'}]_\mathbf{h}$$

[the second line of equation (15)] vanish. No terms with $\mathbf{u}$ are present by definition of the problem. Suppose first that the eikonal function is not adapted to the disturbance, *i.e.* $\varphi = \varphi_0$ is kept. Equation (15) is then reduced to

$$2i\left[\frac{k}{c}\frac{\partial}{\partial t} - \mathbf{k}_\mathbf{h} \cdot \nabla\right]\tilde{\mathbf{A}}_\mathbf{h} = -4\pi r_e \sum_{m,\mathbf{h}'} \tilde{\eta}_{m,\mathbf{h}-\mathbf{h}'}[\exp(i\mathfrak{s}_m) - 1][\tilde{\mathbf{A}}_{\mathbf{h}'}]_\mathbf{h}, \tag{28}$$

directly relating the field-amplitude derivatives to the perturbation terms. The characteristics of this differential equation are the 4-vectors [but written in (1+3) notation], $[-(k/c), \mathbf{k}_\mathbf{h}]$ and, for given boundary conditions, the solutions are fully determined. When dealing separately with temporal and spatial coordinates, as in equation (28), the question may however arise in which way the value of the right-hand side will be distributed among the spatial and the temporal derivatives on the left-hand side. The following discussion will aid in answering that question: Each term $\tilde{\eta}_{m,\mathbf{h}-\mathbf{h}'}[\exp(i\mathfrak{s}_m) - 1]$ in the sum gives a contribution to the change in a given point $(t, \mathbf{r})$ of the phase of $\tilde{\mathbf{A}}_\mathbf{h}$, expressed by the directional derivative along $[-(k/c), \mathbf{k}_\mathbf{h}]$. The contribution from the term $\tilde{\eta}_{m,\mathbf{h}-\mathbf{h}'} \exp(i\mathfrak{s}_m)$ would vanish in a reference frame that is moving along the world line of $\mathfrak{s}_m$, *i.e.* moving along $\mathfrak{k}_m$ with the phase velocity $v_p = \varpi/|\mathfrak{k}|$ of that particular Fourier component of the disturbance (a virtual velocity, which may well be superluminal in the case of an optical phonon at the Brillouin zone center). Since we are staying, instead, in the point $(t, \mathbf{r})$, the phase of the disturbance evolves there. The contribution of $\tilde{\eta}_{m,\mathbf{h}-\mathbf{h}'} \exp(i\mathfrak{s}_m)$ is thus split among the partial derivatives according to the ratio

$$\left(\frac{k}{c}\frac{\partial\tilde{\mathbf{A}}_\mathbf{h}^{(+)}}{\partial t} \cdot \tilde{\mathbf{A}}_{-\mathbf{h}}^{(-)}\right) : [(\mathbf{k}_\mathbf{h} \cdot \nabla\tilde{\mathbf{A}}_\mathbf{h}^{(+)}) \cdot \tilde{\mathbf{A}}_{-\mathbf{h}}^{(-)}] = (\varpi\tau) : \left(\mathfrak{k} \cdot \frac{\mathbf{k}_\mathbf{h}}{|\mathbf{k}_\mathbf{h}|} c\tau\right), \tag{29}$$

where $\mathbf{k}_\mathbf{h}/|\mathbf{k}_\mathbf{h}|$ is a unit vector along $\mathbf{k}_\mathbf{h}$ and $c\tau$ is the distance covered in that direction at the speed of light (of the X-rays) within a time τ. Both parts of the ratio on the left-hand side in equation (29) were multiplied with the same vector $\tilde{\mathbf{A}}_{-\mathbf{h}}^{(-)}$ to yield scalars.

In particular, if the disturbance has high frequencies ϖ at low wavenumbers $|\mathfrak{k}|$, then the time derivative of $\tilde{\mathbf{A}}_\mathbf{h}$ is dominant and a frequency shift may result (heterodyne mixing) – if it is not cancelled by another Fourier component of the disturbance, see below. To further discuss the influence of a disturbance on the field amplitudes, the origin of the Fourier series of the disturbance will be moved to the point $(t, \mathbf{r})$ under consideration. This is, of course, something one should not do when actually calculating a solution of the propagation problem but it is valid in a discussion of local behavior. With the new origin, the dipole approximation can be applied and $\exp(i\mathfrak{s}_m) - 1$ be replaced with $i\mathfrak{s}_m$ in a small region about $(t, \mathbf{r})$. By definition [see equation (5)] therefore, the sum $i\sum_{m,\mathbf{h}'} \tilde{\eta}_{m,\mathbf{h}-\mathbf{h}'}\mathfrak{s}_m$ is real valued. It follows that only the imaginary part of $\tilde{\eta}_{m,\mathbf{h}-\mathbf{h}'}$ actually contributes to the derivatives of $\tilde{\mathbf{A}}_\mathbf{h}$, whereas the real parts of $\tilde{\eta}_{\pm m,\pm(\mathbf{h}-\mathbf{h}')}$ cancel each other out. Therefore, a contribution to the derivatives of the field amplitudes comes only from the inversion antisymmetric part [relative to the origin $(t, \mathbf{r})$] of a disturbance, which may be due to a slope in space or time of the envelope of the disturbance or to the disturbance itself being of noncentrosymmetric character, such as an optical phonon in a noncentrosymmetric crystal (GaAs for example).

Instead of considering only the contribution of a single mode of the disturbance with a particular frequency ϖ and wavevector $\mathfrak{k}$, one might also consider wavepackets of optical phonons. If the group velocity of such a wavepacket matches the group velocity of the diffracting X-rays, then the action of the disturbance on the X-rays will be enhanced (Entin, 1978). One may interpret a frequency shift under these conditions as a constructive superposition of Doppler shifts upon reflection from vibrating lattice planes in phase with the X-rays bouncing back and forth in a *Pendellösung* oscillation. This bouncing motion is, of course, a continuous scattering process from lattice planes moving synchronously with the *Pendellösung* oscillation. According to equation (28), the magnitude of this shift may be estimated as the optical phonon energy transferred to the X-rays within a multiple M of *Pendellösung* periods given by the ratio of vibration amplitude *versus* lattice parameter. If this ratio is 0.1 (about the maximum permitted by the Lindeman criterion of lattice stability), then an optical phonon energy of typically 10 to 100 meV is taken up by the X-rays within 10 *Pendellösung* periods.

One final point: the eikonal function was kept unchanged from φ_0 in the above discussion. If φ is now adapted to minimize the derivatives in the presence of the disturbance, then the derivatives of $\tilde{\mathbf{A}}_\mathbf{h}$ become smaller and the phase shifts (frequency shifts and wavevector changes) represented by them are taken up by $\dot{\varphi}$ and $\nabla(\varphi - \varphi_0)$. Nothing (except perhaps a higher accuracy of the solution) changes in the actual behavior of the waves (frequency shifts *etc.*) by doing so.

13. From boundary to transition conditions

In analogy to the boundary conditions for the coupling of waves across a crystal boundary, the transport of waves within a disturbed crystal is also subject to the requirement of continuity. This continuity is expressed in terms of gradients instead of the vectorial algebraic relations at a discontinuous boundary. Generally, these gradients are taken in space–time, as illustrated in Fig. 6. For the purposes of the local behavior of a solution of equation (15), such as in the transition of a disturbed layer, one may look at one of two complementary aspects of the modulated Bloch wave. (i) When the eikonal function is left unchanged, then all the effects of the disturbance are taken up by the field amplitudes. This is demonstrated in §10 in the discussion of interbranch scattering. This approach is analogous to the splitting of amplitudes among the branches of the dispersion surface in the transition of a discontinuous interface between a perfect crystal and an amorphous medium (or beteen two perfect crystals). Instead, (ii) one may also leave the field amplitudes unchanged and study the changes in the eikonal function as an interface is traversed. This is the approach that was taken in the derivation of equation (17). In doing so, one focuses the attention on the changes in the wavevectors, similar to wavevector matching across perfect crystal boundaries. As stated towards the end of §10, a global minimization of the merit function will yield a result somewhere between these two extremes, trading a change in amplitudes at a particular location (and thus incurring a penalty in the merit function) for a better fit somewhere else.

Fig. 6 shows the dispersion surface of a two-wave case before and after the passage of a disturbance, which reduces the structure factor relevant to the diffraction. The expressions 'before' and 'after' are used here in the sense of a time-like separation. The dispersion surface of the undisturbed crystal [indicated by ②] has a larger gap between its branches than the one in effect after ① the disturbance has passed.

Before the disturbance, a mode was excited on the α branch, indicated by the ellipse ②. The disturbance leads to interbranch scattering, and the amplitudes are reassigned among the new (closer spaced) α and β branches along the space–time gradient of the disturbance, which is indicated by the straight line connecting the ellipses for the original mode ② and the new modes. Because the space-time gradient of the disturbance has a component along the vertical axis of the figure, which corresponds to the photon energy, a frequency shift of the diffracting X-rays occurs. As pointed out above, this requires a change in the crystal structure of a noncentrosymmetric character. That does, however, not mean that the crystal structure long before and long after the disturbance needs to differ in its degree of centrosymmetry: the space–time envelope of the structure change itself provides a noncentrosymmetry. This is quite different from a situation where coherent optical phonons are present in a stationary manner. To obtain a frequency shift in such a case, the optical phonons themselves must change the degree of centrosymmetry.

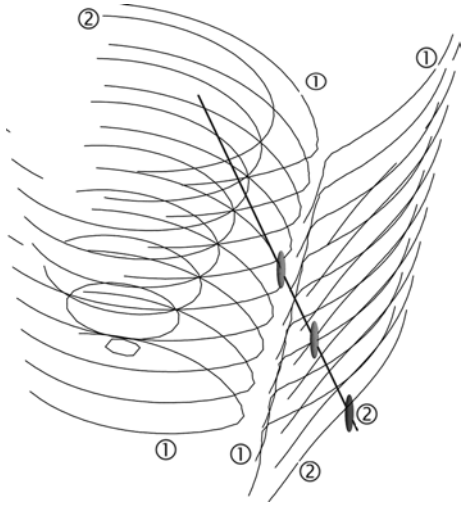

Figure 6
Dispersion surfaces before (wider spaced pair) and after (closer spaced pair) the passage of a disturbance that reduces the structure factor associated with a particular reciprocal-lattice vector **H**. The perspective is about the same as in Fig. 1. Also shown is the space–time gradient of the disturbance and the redistribution of waves among the branches of the dispersion surface. See text.

14. Conclusions

The next generation of X-ray sources, particularly the XFELs, will provide exciting new opportunities in the study of ultrafast processes. A theoretical basis needs to be developed to fully exploit these opportunities, to understand X-ray diffraction in laser pump, X-ray probe experiments, to develop ultrafast X-ray instrumentation and to describe the diffraction of intense femtosecond X-ray beams that modify the crystal as they propagate. The theory presented here was developed with these goals in mind. It is formulated in a unified space–time picture to make it applicable to time scales of the order of the X-ray/lattice interaction time. Dynamical diffraction theory is usually based upon macroscopic electromagnetism, using the quantities χ and $\mathbf{D}$, which are derived from microscopic electromagnetism in a spatial averaging procedure. In cases where the spatial frequencies of a disturbance are not negligible relative to the X-ray wavenumber, the assumption of the availability of a suffiently large averaging volume becomes invalid. If the disturbance contains only a single spatial frequency, this problem can be addressed through a suitably modified crystal unit cell. However, nonperiodic (wave-packet type *etc.*) disturbances cannot be dealt with in this way. The same holds true for disturbances, whose characteristic times correspond to such spatial frequencies at the speed of light, and particularly for applications in the diffractive femtosecond manipulation of X-rays with laser-induced disturbances traveling through a crystal at nearly the speed of light. For this reason, the theory is presented here on the basis of microscopic electromagnetism.

APPENDIX *A*
The transverse current

To compute the transverse current, equation (2), from equation (7), the spatial dependences of $\tilde{\mathbf{A}}_{\mathbf{h}}$, $S_{n,\mathbf{h}}$ (through φ and $\mathbf{u}$) and $\mathfrak{s}_m$ (through $\mathbf{u}$) can be expressed in Taylor expansions:

$$\mathbf{h}\cdot\mathbf{u}(\mathbf{r}',t)=\mathbf{h}\cdot\mathbf{u}(\mathbf{r},t)+(\mathbf{r}'-\mathbf{r})\cdot\nabla\mathbf{u}|_{\mathbf{r}}\cdot\mathbf{h}+\ldots \quad (30)$$

$$\varphi(\mathbf{r}',t)=\varphi(\mathbf{r},t)+(\mathbf{r}'-\mathbf{r})\cdot\nabla\varphi|_{\mathbf{r}}+\ldots \quad (31)$$

$$\tilde{\mathbf{A}}_{\mathbf{h}'}(\mathbf{r}',t)=\tilde{\mathbf{A}}_{\mathbf{h}'}(\mathbf{r},t)+(\mathbf{r}'-\mathbf{r})\cdot\nabla\tilde{\mathbf{A}}_{\mathbf{h}'}|_{\mathbf{r}}+\ldots, \quad (32)$$

which yield (using the variable substitution $\mathbf{r}'-\mathbf{r}=\mathbf{r}''$):

$$\begin{aligned}\mathbf{J}_t(\mathbf{r},t)=-\frac{r_e c}{4\pi}\sum_{\substack{mn\\ \mathbf{h}\mathbf{h}'}}\tilde{\eta}_{m,\mathbf{h}-\mathbf{h}'}\exp[-i(\omega+\varpi m)t]\\ \times\nabla\times\nabla\times\Bigg(\exp\{i[\mathbf{r}\cdot(\mathbf{k}_{\mathbf{h}}+\mathfrak{k}_m)+\varphi_n-\mathbf{h}\cdot\mathbf{u}]\}\\ \times\int\mathrm{d}\mathbf{r}''\frac{\tilde{\mathbf{A}}_{\mathbf{h}'}(\mathbf{r})+\mathbf{r}''\cdot\nabla\tilde{\mathbf{A}}_{\mathbf{h}'}|_{\mathbf{r}}}{|\mathbf{r}''|}\\ \times\exp\{i[\mathbf{r}''\cdot(\mathbf{k}_{\mathbf{h}^\circ}+\mathfrak{k}_m+\nabla\varphi_n)]\}\Bigg)\end{aligned} \quad (33)$$

Integration of the first term, $\tilde{\mathbf{A}}_{\mathbf{h}'}(\mathbf{r})$, in the sum can be done by aligning the z axis of cylindrical (φ,r,z) coordinates along $\mathfrak{K}_{\mathbf{h},m}=\mathbf{k}_{\mathbf{h}^\circ}+\mathfrak{k}_m+\nabla\varphi$ (abbreviated further as $\mathfrak{K}$ where possible) and using equation (3.754.2) of Gradshtein & Ryzhik (1981) for the z integration, followed by equation (6.561.16) of Gradshtein & Ryzhik (1981) for the r integration. The result is $|4\pi\tilde{\mathbf{A}}_{\mathbf{h}'}(\mathbf{r})/\mathfrak{k}_{\mathbf{h},m}|^2$.

Some more effort is required for the $\mathbf{r}''\cdot\nabla\tilde{\mathbf{A}}_{\mathbf{h}'}$ term. First, $\nabla\tilde{\mathbf{A}}_{\mathbf{h}'}$ is split into a longitudinal gradient part $\mathfrak{k}(\mathfrak{K}\cdot\nabla\tilde{\mathbf{A}}_{\mathbf{h}'})/|\mathfrak{K}|^2$ and a transverse remainder. The integral over the latter vanishes owing to symmetry in the (φ,r) integration in the above cylindrical coordinates. For the former, an exponential damping factor $\exp(-\mu|z|)$ is introduced with the limit $\mu\to 0$ taken below. This makes the integral over $\mathbf{r}''\cdot\nabla\tilde{\mathbf{A}}_{\mathbf{h}'}|_{\mathbf{r}}\exp(i\mathfrak{K}\cdot\mathbf{r}'')/|\mathbf{r}''|$:

$$\begin{aligned}2\pi\frac{(\mathfrak{K}\cdot\nabla\tilde{\mathbf{A}}_{\mathbf{h}'})}{|\mathfrak{K}|}\int_0^\infty r\,\mathrm{d}r\Bigg(\int_{-\infty}^0\frac{z\exp[(i|\mathfrak{K}|+\mu)z]}{(r^2+z^2)^{1/2}}\,\mathrm{d}z\\ +\int_0^\infty\frac{z\exp[(i|\mathfrak{K}|-\mu)z]}{(r^2+z^2)^{1/2}}\,\mathrm{d}z\Bigg).\end{aligned} \quad (34)$$

The first ($-\infty$ to 0) of these two integrals is the negative complex conjugate of the other. With equation (3.366.3) of Gradshtein & Ryzhik (1981), the integral (34) becomes:

$$i\pi^2\frac{(\mathfrak{K}\cdot\nabla\tilde{\mathbf{A}}_{\mathbf{h}'})}{|\mathfrak{K}|}\int_0^\infty r^2\,\mathrm{d}r\,\Im\{\mathbf{H}_1[(\mu-i|\mathfrak{K}|)r]-Y_1[(\mu-i|\mathfrak{K}|)r]\}, \quad (35)$$

where $\Im$ denotes the imaginary part and $\mathbf{H}_1$ and Y_1 are Struve and Bessel functions, respectively. The r integral converges only in the limit $\mu\to 0$ (shown below), and is thus not to be found in a reference table of integrals (Gradshtein & Ryzhik, 1981). However, convergence can be determined through an asymptotic expansion of $\mathbf{H}_1(z)-Y_1(z)$ for large z [Abramowitz & Stegun, 1984, equation (12.1.31)]:

$$\mathbf{H}_1(z)-Y_1(z)\sim\frac{2}{\pi}\left[1+\frac{1}{z^2}-\frac{1^2\times 3}{z^4}+\frac{1^2\times 3^3\times 5}{z^6}-\ldots\right]. \quad (36)$$

The first term, 1, in the series does not contribute to the imaginary part and the terms with z^{-4}, $z=(\mu-i|\mathfrak{K}|)r$ and beyond (multiplied by r^2 in the integral) are all integrable. That leaves only the z^{-2} term, which is real valued for purely imaginary z. Therefore, the integral (35) converges in the limit $\mu\to 0$ and

$$\int\mathrm{d}\mathbf{r}''\frac{\mathbf{r}''\cdot\nabla\tilde{\mathbf{A}}_{\mathbf{h}'}|_{\mathbf{r}}}{|\mathbf{r}''|}\exp(i\mathbf{r}''\cdot\mathfrak{K}_{\mathbf{h},m})\approx i\frac{\pi^2(\mathfrak{K}_{\mathbf{h},m}\cdot\nabla\tilde{\mathbf{A}}_{\mathbf{h}'})}{|\mathfrak{K}_{\mathbf{h},m}|^4}\times 1.273, \quad (37)$$

where the number $1.273\approx 4/\pi$ comes from a numeric integration of $r^2\Im[\mathbf{H}_1(ir)-Y_1(ir)]$ over the interval $[0,\ldots,20]$.

We have thus

$$\mathbf{J}_t(\mathbf{r},t) = -r_e c \sum_{\substack{mn\\ \mathbf{h}\mathbf{h}'}} \tilde{\eta}_{m,\mathbf{h}-\mathbf{h}'} \times \nabla \times \nabla \times \left[\left(\frac{\tilde{\mathbf{A}}_{\mathbf{h}'}}{|\mathfrak{K}_{\mathbf{h},m}|^2} + i\frac{(\mathfrak{K}_{\mathbf{h},m}\cdot\nabla\tilde{\mathbf{A}}_{\mathbf{h}'})}{|\mathfrak{K}_{\mathbf{h},m}|^4}\right) \times \exp[i(S_{n,\mathbf{h}}+\mathfrak{s}_m)]\right]. \quad (38)$$

Application of the $\nabla\times\nabla\times$ operator to the $\tilde{\mathbf{A}}_{\mathbf{h}'}$ term leads to

$$\nabla\times\nabla\times\tilde{\mathbf{A}}_{\mathbf{h}} + 2i\mathfrak{K}\times(\nabla\times\tilde{\mathbf{A}}_{\mathbf{h}}) + i\nabla\times(\mathfrak{K}\times\tilde{\mathbf{A}}_{\mathbf{h}}) + \mathfrak{K}\times\tilde{\mathbf{A}}_{\mathbf{h}}\times\mathfrak{K}$$

(with the indices $\mathbf{h}, m, n$ of $\mathfrak{K}$ suppressed). The term $\nabla\times(\mathfrak{K}\times\tilde{\mathbf{A}}_{\mathbf{h}'})$ can be converted to $\mathfrak{K}(\nabla\cdot\tilde{\mathbf{A}}_{\mathbf{h}'}) - \nabla(\mathfrak{K}\cdot\tilde{\mathbf{A}}_{\mathbf{h}'})$ using the vector formulas

$$\nabla\times(\mathbf{a}\times\mathbf{b}) = \mathbf{a}\times(\nabla\times\mathbf{b}) - \mathbf{b}\times(\nabla\times\mathbf{a}) + (\mathbf{b}\times\nabla)\times\mathbf{a} - (\mathbf{a}\times\nabla)\times\mathbf{b}$$

and

$$\nabla(\mathbf{a}\cdot\mathbf{b}) = \mathbf{a}(\nabla\cdot\mathbf{b}) + \mathbf{b}(\nabla\cdot\mathbf{a}) + (\mathbf{a}\times\nabla)\times\mathbf{b} + (\mathbf{b}\times\nabla)\times\mathbf{a},$$

which can be found on the web (Piché, 2003) or can be derived from the formulas on the inside cover of Jackson (1975) by use of $\mathbf{a}\times(\nabla\times\mathbf{b}) - (\mathbf{a}\times\nabla)\times\mathbf{b} = \mathbf{a}(\nabla\cdot\mathbf{b}) - (\mathbf{a}\cdot\nabla)\mathbf{b}$. This gives the last of the three terms in equation (11). In a purely transverse wave, both $\nabla\cdot\tilde{\mathbf{A}}_{\mathbf{h}'}$ and $\mathfrak{K}\cdot\tilde{\mathbf{A}}_{\mathbf{h}'}$ vanish. However, as pointed out in Appendix *D*, the individual Bloch waves may develop longitudinal components as they propagate into a distorted lattice. After neglecting the second-order derivative of $\tilde{\mathbf{A}}_{\mathbf{h}}$, the transverse current is

$$\mathbf{J}_t = -r_e c \sum_{\substack{mn\\ \mathbf{h}\mathbf{h}'}} \tilde{\eta}_{m,\mathbf{h}-\mathbf{h}'}\left([\tilde{\mathbf{A}}^{(m)}_{\mathbf{h}'}]_{\mathbf{h}} + i\frac{[\nabla\tilde{\mathbf{A}}^{(m)}_{\mathbf{h}'}]_{\mathbf{h}}}{k}\right)\exp[i(S_{n,\mathbf{h}}+\mathfrak{s}_m)], \quad (39)$$

where the definitions of $\mathfrak{s}_m$ and $S_{n,\mathbf{h}}$ are given in equations (8) and (5), respectively, and $[\tilde{\mathbf{A}}^{m}_{\mathbf{h}'}]_{\mathbf{h}}$ and $[\nabla\tilde{\mathbf{A}}^{(m)}_{\mathbf{h}'}]_{\mathbf{h}}$ are defined in equations (10) and (11).

To identify the contribution of $\mathfrak{K}_{\mathbf{h},m}\cdot\nabla\tilde{\mathbf{A}}_{\mathbf{h}'}$ to $\mathbf{J}_t$, one may define a longitudinal part $\nabla\tilde{\mathbf{A}}^{\parallel}_{\mathbf{h}'} = (\nabla\mathbf{A}_{\mathbf{h}'}\cdot\mathfrak{K}_{\mathbf{h},m})(\mathfrak{K}_{\mathbf{h},m})/|\mathfrak{K}_{\mathbf{h},m}|^2$ of the vector potential and split $\nabla\tilde{\mathbf{A}}_{\mathbf{h}'} = \nabla\mathbf{A}^{\perp}_{\mathbf{h}'} + \nabla\mathbf{A}^{\parallel}_{\mathbf{h}'}$. Application of the operator $\nabla\times\nabla\times$ to $\mathfrak{K}_{\mathbf{h},m}\cdot\nabla\tilde{\mathbf{A}}^{\parallel}_{\mathbf{h}'}\exp[i(S_{n,\mathbf{h}}+\mathfrak{s}_m)]$, and keeping only first-order derivatives of $\tilde{\mathbf{A}}_{\mathbf{h}'}$, yields zero, and $\nabla\tilde{\mathbf{A}}^{\perp}_{\mathbf{h}'}$ may be split again into a longitudinal gradient part $\mathfrak{K}_{\mathbf{h},m}(\mathfrak{K}_{\mathbf{h},m}\cdot\nabla\tilde{\mathbf{A}}^{\perp}_{\mathbf{h}'})/|\mathfrak{K}_{\mathbf{h},m}|^2$ and a transverse remainder. As above, before equation (34), the latter vanishes owing to symmetry in the (φ, r) integration. In summary, the contribution to the transverse current comes from the longitudinal gradient part of the transverse part of the vector potential. Its magnitude is given by the directional derivative of $\tilde{\mathbf{A}}_{\mathbf{h}}$ in equation (12), and thus depends on the diffraction process in the crystal. In contrast, the transverse gradient part of the vector potential is given by the boundary conditions, and may be much larger than the longitudinal gradient part. It does, however, not contribute to the transverse current.

APPENDIX *B*
Microscopic or macroscopic electromagnetism

The dynamical theory of X-ray diffraction is usually derived in terms of macroscopic electromagnetism, such as the electric susceptibility χ and polarization $\mathbf{P}$. The wave equation then reads

$$\nabla^2\mathbf{D} - \frac{1}{c^2}\frac{\partial^2\mathbf{D}}{\partial t^2} + 4\pi\nabla\times\nabla\times(\chi\mathbf{D}) = 0, \quad (40)$$

with $\mathbf{D} = \mathbf{E} + 4\pi\mathbf{P}$.

In analogy to equations (5) and (6), χ is now represented by a sum of Bloch waves [replace $\tilde{\eta}_{m,\mathbf{h}}$ in equation (5) with $\tilde{\chi}_{m,\mathbf{h}}$] and $\mathbf{D}$ as a modulated Bloch wave [replace $\tilde{\mathbf{A}}_{\mathbf{h}}(\mathbf{r},t)$ in equation (6) with $\tilde{\mathbf{D}}_{\mathbf{h}}(\mathbf{h},t)$].

These Bloch waves may now be inserted into equation (40). Keeping only the leading-order terms, as in the derivation of equation (12), gives:

$$2i\left(\frac{k}{c} - \frac{\dot{\varphi}}{c^2} + \frac{\dot{\mathbf{u}}\cdot\mathbf{h}}{c^2}\right)\frac{\partial\tilde{\mathbf{D}}_{\mathbf{h}}}{\partial t} - 2i(\mathbf{k}_{\mathbf{h}^\circ}+\nabla\varphi)\cdot\nabla\tilde{\mathbf{D}}_{\mathbf{h}} = \left[\left(k - \frac{\dot{\varphi}}{c} + \frac{\dot{\mathbf{u}}\cdot\mathbf{h}}{c}\right)^2 - (\mathbf{k}_{\mathbf{h}^\circ}+\nabla\varphi)^2\right]\tilde{\mathbf{D}}_{\mathbf{h}} + 4\pi k^2\sum_{m,\mathbf{h}'}\chi_{m,\mathbf{h}-\mathbf{h}'}\exp(i\mathfrak{s}_m)[\tilde{\mathbf{D}}_{\mathbf{h}'}]_{\mathbf{h}}, \quad (41)$$

where

$$[\tilde{\mathbf{D}}_{\mathbf{h}'}]_{\mathbf{h}} = \frac{(\mathbf{k}_{\mathbf{h}^\circ}+\mathfrak{k}_m+\nabla\varphi)\times\tilde{\mathbf{D}}_{\mathbf{h}'}\times(\mathbf{k}_{\mathbf{h}^\circ}+\mathfrak{k}_m+\nabla\varphi)}{k^2} \quad (42)$$

is defined to correspond to $[\tilde{\mathbf{A}}_{\mathbf{h}'}]_{\mathbf{h}}$ in equation (10). There is, however, one important difference between the two: where equation (10) has a denominator $|\mathbf{k}_{\mathbf{h}^\circ}+\mathfrak{k}_m+\nabla\varphi|^2$, equation (42) has only k^2. Because the denominator involves the Bloch component wavevectors $\mathbf{k}_{\mathbf{h}^\circ}$, it is not possible to deal with this problem by simply defining a modified susceptibility. The difference between the denominators becomes relevant when $|\mathfrak{k}_m|$ is not negligible in comparison to $|\mathbf{k}_{\mathbf{h}^\circ}|$, such as, for example, in short-period superstructures or laser-induced optical phonons. Laser wavelengths typically being longer than those of X-rays by a factor of *ca* 10^4, the optical phonons excited in a linear-response material have wavevectors $|\mathfrak{k}_m| < 10^{-4}|\mathbf{k}_{\mathbf{h}^\circ}|$. However, considerably larger phonon wavenumbers may be obtained with a crystal that exhibits a nonlinear response to a driving laser field, for example close to a ferroelectric phase transition. This may be a rather rare case, but a potentially very important one for practical applications.

The underlying reason for the difference between the denominators of equations (10) and (42) is that the concept of an electric susceptibility is a macroscopic one, derived from microscopic electromagnetism in a spatial averaging procedure (Jackson, 1975) or, in the case of a periodic electron density, through a Fourier integration. When the spatial frequencies $\mathfrak{k}_m$ of a disturbance are not negligible relative to the X-ray wavenumber k, *i.e.* when the disturbance is noticeable within the averaging volume, then a microscopic derivation yields a result that is at variance with the macroscopic

one, and the former must be given precedence. When looking at this point from a formal point of view, the wavevectors $\mathfrak{k}_m$ of the disturbances appear in the exponent in the integrand of equation (33). Because they do so in a vector sum with $\mathbf{k}_{\mathbf{h}^\circ} + \nabla\varphi$, the integral depends on $\mathbf{k}_{\mathbf{h}^\circ}$. In contrast, a spatial averaging procedure to define a susceptibility would not exhibit this dependence on $\mathbf{k}_{\mathbf{h}^\circ} + \nabla\varphi$.

APPENDIX *C*
Elementary interaction length and time

The most fundamental interaction length is the classical electron radius r_e in the case of Thomson scattering and the atom diameter in the case of resonant X-ray scattering. Likewise, the intrinsic interaction time τ_0 of Thomson scattering is the reciprocal electron rest energy (*i.e.* $\tau_0 = 2\pi\hbar/511\,\mathrm{keV}$) and the fundamental interaction time of resonant scattering is the smaller of the reciprocal energy offset from exact resonance and the lifetime of the intermediate excited state. However, each individual scattering event from an electron or an atom contributes only a small amplitude. In a perfect crystal, these amplitudes add up coherently until, after passage of a large number of atoms (typically 10^5 or more), the scattered amplitudes are equal in magnitude to the original wave(s) and thus have a sizeable influence. The interaction of the X-rays with a perfect crystal therefore occurs over a characteristic length of many ($\sim 10^5$ or more) interatomic distances. A good measure of the interaction length is one-half of the *Pendellösung* length of the Laue case (Batterman & Cole, 1964; Authier, 2001), which is the length required for complete amplitude swapping among the diffracting waves. Likewise, the lattice interaction time is the time it takes for the many distributed microscopic scattering events to build up a strong scattered amplitude, *i.e.* the time the X-rays take to traverse the lattice interaction length. With a strong structure factor, such as Si (111), and photons of 12.4 keV, the *Pendellösung* length is about 30 μm, and the time corresponding to one-half of that is about 50 fs. With weaker structure factors, the interaction lengths and times are correspondingly longer. In comparison, optical phonon oscillation periods are typically of the order of 100 to 200 fs. There is, however, a way to change a crystal's diffractive power even faster than that, using a massive electronic excitation from the valence band of a semiconductor to its conduction band. In the complementary picture of bonds (Phillips, 1973), this is equivalent to a conversion from bonding to antibonding orbitals. In diamond, four out of six electrons are in the valence structure and thus directly accessible to laser excitation, and the diffractive power can thus be made to change drastically within a few femtoseconds.

In a perfect crystal, the dispersion surface (Batterman & Cole, 1964; Authier, 2001) has well defined branches, which may be considered separately in the description of diffractive X-ray propagation. The *Pendellösung* phenomenon is due to a beating of modes originating from the branches, and each mode in itself does not exhibit any characteristic interaction length or time. In fact, X-rays in a mode on the dispersion surface do not interact with the lattice at all because the scattering from the electrons is built into the definition of the mode. When considering X-rays in terms of other modes of the electromagnetic field, for example by using wavevectors originating from the symmetry center of the dispersion hyperbola (see Fig. 4, lower right-hand graph), then these X-rays do scatter from the lattice. The interaction of X-rays with a lattice is thus a matter of the point of view taken.

The wavevectors of modes on different branches of the dispersion surface have extremal (maximal and minimal) lengths under given boundary conditions,[1] and differences between them become apparent in the form of a 2π phase shift upon traversal of the *Pendellösung* period. A deviation from perfect-crystal-like diffraction will thus occur when a disturbance has the effect of inducing a noticeable change (most of all in the phases) in the Bloch-wave amplitudes $\tilde{\mathbf{A}}_{\mathbf{h}}$ within the *Pendellösung* length, or the corresponding time. This can generally be expected to occur if the diffractive properties of the crystal change over these length and time scales. It is then not possible to define a dispersion surface in the strict sense (only approximate it, which is what most of this text is about), and the X-rays in any applicable mode of the electromagnetic field do interact with the lattice throughout their propagation.

When the crystal's diffractive power changes only slightly within the lattice interaction length and time, then an adiabatic approximation may be used, *i.e.* the propagation of X-rays may be described in terms of a succession of perfect-crystal solutions. This is the approach of the eikonal approximation. When, at the other extreme, a spatial disturbance occurs on a length scale that is much shorter than the lattice interaction length, then perfect-crystal solutions may be joined algebraically to each other. This is done, for example, when wavevectors and amplitudes are matched across a surface of a perfect crystal. Likewise, a very sudden change relative to the lattice interaction time can be dealt with algebraically. However, if the changes occur on length or time scales that are comparable to the lattice interaction length or time, then a fully wave–optical treatment becomes necessary.

The most challenging case is that of a spatio-temporal disturbance of the crystal that is comparable to both the lattice interaction length and the lattice interaction time. This kind of disturbance is highly interesting for the ultrafast manipulation of X-rays (Adams, 2002), which requires careful group-velocity matching. To handle this case, the theory should treat spatial and temporal coordinates in the same way.

APPENDIX *D*
Beyond the leading order

Practical applications in the subpicosecond manipulation of X-rays may require very strong disturbances to the crystal structure, making it necessary to go beyond the leading-order perturbation terms.

[1] The dispersion hyperbola of the two-wave case may be derived from Fermat's principle, with minimal and maximal optical path lengths simultaneously present (Adams, 1989).

One direction to explore is indicated at the end of §2: a rapid change of the electron density implies a high velocity of the electrons. Suppose, for example, that the electrons in a noncentrosymmetric crystal are delocalized within 3 fs. This means that there is a net motion of electrons (*i.e.* an unbalanced current) of, say, 1 Å in 3 fs, and the resulting velocity is 3×10^4 m s^{-1}, or 10^{-4} of the speed of light, making the Lorentz force marginally relevant.

Another issue is higher-order terms because equation (12) was derived using only the leading-order terms of the disturbance and of $\tilde{\mathbf{A}}$. To estimate the relative importance of the next-to-leading-order terms identified just before equation (12), *i.e.* (i) second-order derivatives of $\tilde{\mathbf{A}}$, (ii) products of first-order derivatives of $\mathbf{u}$ and φ with first-order derivatives of $\tilde{\mathbf{A}}$, and (iii) first-order derivatives of $\tilde{\mathbf{A}}$ multiplied with a Bloch component of the electron density, consider the following: according to equation (12), $\nabla\tilde{\mathbf{A}}_{\mathbf{h}}$ scales as $(\nabla\mathbf{u}\cdot\mathbf{h})\tilde{\mathbf{A}}_{\mathbf{h}}$ and $(r_e\eta_{\mathbf{h}-\mathbf{h}'}/k)\tilde{\mathbf{A}}_{\mathbf{h}'}$. Taking the gradient of all of these, we see that the terms of types (i) to (iii) are all of roughly the same order of magnitude, *i.e.* not apart from each other by an order of the derivatives or a factor $r_e\eta/k^2 \approx 10^{-6}$. An extension of equation (12) to include the next-to-leading-order terms will thus have to include types (i) to (iii) and, in particular, all of equation (11). The last term of that equation deserves some special attention: in the course of propagation, the field amplitudes may develop a slight longitudinal component because equation (10) results in a vector that is transverse to $\mathbf{k}_{\mathbf{h}^\circ} + \mathfrak{k}_m + \nabla\varphi$, and not to the wavevector $\mathbf{k}_{\mathbf{h}^\circ} + \nabla\varphi$ of $\tilde{\mathbf{A}}_{\mathbf{h}}$. Furthermore, equation (10) is defined locally and a changing lattice orientation due to a displacement field $\mathbf{u}$ also contributes to longitudinal components. These longitudinal components are of no consequence if only the leading-order terms are considered. If, however, the next-to-leading-order terms are also taken into account, then a longitudinal component of $\tilde{\mathbf{A}}_{\mathbf{h}}$ may enter through the last term in equation (11).

This work was supported in part by the US Department of Energy under contract W-31-109-ENG-38.

References

Abramowitz, M. & Stegun, I. (1984). *Handbook of Mathematical Functions.* New York: Dover.

Adams, B. (1989). Diploma thesis, University of Munich, Germany.

Adams, B. (2002). *SPIE Proc.* **4500**, 89–100.

Adams, B. (2003). Editor. *Nonlinear Optics, Quantum Optics and Ultrafast Pheneomena with X-rays.* Boston: Kluwer Academic Publishers.

Adams, B., Fernandez, P., Lee, W.-K., Materlik, G., Mills, D. & Novikov, D. (2000). *J. Synchrotron Rad.* **7**, 81–88.

Ashcroft, N. & Mermin, N. (1976). *Solid State Physics.* Singapore/South Melbourne/Toronto/London/Colonia Polanco (Mexico)/Madrid: Thomson Learning, Inc.

Authier, A. (2001). *Dynamical Theory of X-ray Diffraction.* Oxford: Great Clarendon Press.

Authier, A. & Balibar, F. (1970). *Acta Cryst.* A**26**, 647–654.

Balibar, F. (1969). *Acta Cryst.* A**25**, 650–658.

Balibar, F., Chukhovskii, F. & Malgrange, C. (1983). *Acta Cryst.* A**39**, 387–399.

Balibar, F., Epelboin, Y. & Malgrange, C. (1975). *Acta Cryst.* A**31**, 836–840.

Batterman, B. & Cole, H. (1964). *Rev. Mod. Phys.* **36**, 681–716.

Bilderback, D., Bazarov, I., Finkelstein, K., Gruner, S., Krafft, G., Merminga, L., Padamsee, H., Shen, Q., Sinclair, C., Tigner, M. & Talman, R. (2001). *Synchrotron Radiat. News*, **14**, 12–21.

Bilderback, D. H., Bazarov, I. V., Finkelstein, K., Gruner, S. M., Padamsee, H. S., Sinclair, C. K., Shen, Q., Talman, R., Tigner, M., Krafft, G. A. & Merminga, L. (2003). *J. Synchrotron Rad.* **10**, 346–348.

Bishop, R. & Goldberg, S. (1968). *Tensor Analysis on Manifolds.* New York: Dover Publications.

Bonse, U. (1964). *Z. Phys.* **177**, 385–423.

Bonse, U. & Graeff, W. (1973). *Z. Naturforsch. Teil A*, **28**, 558–564.

Chukhovskii, F. & Förster, E. (1995). *Acta Cryst.* A**51**, 668–672.

Davis, T. (1995). *Acta Cryst.* A**51**, 354–360.

Entin, I. (1978). *Sov. Phys. Solid State*, **20**, 754–756.

Entin, I. & Assur, K. (1981). *Acta Cryst.* A**37**, 769–774.

Gradshtein, I. & Ryzhik, I. (1981). *Tables of Series, Products, and Integrals.* Thun: Harri Deutsch.

Graeff, W. (2002). *J. Synchrotron Rad.* **9**, 293–297.

Jackson, J. (1975). *Classical Electrodynamics*, 2nd ed. New York: John Wiley and Sons.

Kato, N. (1958). *Acta Cryst.* **11**, 885–887.

Kato, N. (1963). *J. Phys. Soc. Jpn*, **18**, 1785–1791.

Kato, N. (1964*a*). *J. Phys. Soc. Jpn*, **19**, 67–77.

Kato, N. (1964*b*). *J. Phys. Soc. Jpn*, **19**, 971–985.

Kato, N. (1973). *Z. Naturforsch. Teil A*, **28**, 604–609.

Kato, N. (1980*a*). *Acta Cryst.* A**36**, 763–769.

Kato, N. (1980*b*). *Acta Cryst.* A**36**, 770–778.

Krejcik, P., Arthur, J., Carr, R., Cornacchia, M., Emma, P., Iversen, R., Safranek, J. & Tatchyn, R. (2001). Proc. ICFA 2001, http://www.stonybrook.edu/icfa2001/Papers/w4-2.pdf.

Kulda, J. (1984). *Acta Cryst.* A**40**, 120–126.

Laue, M. von (1952). *Acta Cryst.* **5**, 619–625.

Materlik, G. & Tschentscher, T. (2001). Editors. *Welcome to the TESLA Technical Design Report*, Part V, DESY, Germany, http://tesla.desy.de/new_pages/TDR_CD/PartV/fel.html.

Neutze, R., Wouts, R., van der Spoel, D., Weckert, E. & Hajdu, J. (2000). *Nature (London)*, **406**, 752–757.

Okkerse, B. & Penning, P. (1963). *Philips Res. Rep.* **18**, 82–94.

Penning, P. & Polder, D. (1961). *Philips Res. Rep.* **16**, 419–440.

Phillips, J. (1973). *Bands and Bonds in Semiconductors.* New York/London: Academic Press.

Piché, R. (2003). *Vector Analysis Formulas*, Tampere University of Technology, http://matwww.ee.tut.fi/~piche/fields/formulas.html.

Schoenlein, R., Chattopadhyay, S., Chong, H., Glover, T., Heimann, P., Leemans, W., Shank, C., Zholents, A. & Zolotorev, M. (2000). *Appl. Phys. B*, **71**, 1–10.

Schoenlein, R., Chattopadhyay, S., Chong, H., Glover, T., Heimann, P., Shank, C., Zholents, A. & Zolotorev, M. (2000). *Science*, **287**, 2237–2240.

Shastri, S., Zambianchi, P. & Mills, D. (2001). *J. Synchrotron Rad.* **8**, 1131–1135.

Sondhauss, P. & Wark, J. (2003). *Acta Cryst.* A**59**, 7–13.

Takagi, S. (1962). *Acta Cryst.* **15**, 1311–1312.

Takagi, S. (1969). *J. Phys. Soc. Jpn*, **26**, 1239–1253.

Taupin, D. (1964). *Bull. Soc. Fr. Minéral. Cristallogr.* **87**, 469–511.

Wark, J. & He, H. (1994). *Laser Particle Beams*, **12**, 507–513.

Wark, J. & Lee, R. (1999). *J. Appl. Cryst.* **32**, 692–703.

Zolotoyabko, E. & Panov, V. (1992). *Acta Cryst.* A**48**, 225–231.

Zolotoyabko, E., Polikarpov, I., Panov, V. & Schvarkov, D. (1992). *J. Appl. Cryst.* **25**, 88–91.

Zolotoyabko, E. & Sander, B. (1995). *Acta Cryst.* A**51**, 163–171.

Zolotoyabko, E., Sander, B., Komem, Y. & Kantor, B. (1994). *Acta Cryst.* A**50**, 253–257.